Annual Report

Authors

Ron Adamson
Zircology Plus, Fremont, CA, USA

Friedrich Garzarolli
Fürth, Germany

Charles Patterson
Clovis, CA, USA

Peter Rudling
ANT International, Skultuna, Sweden

Alfred Strasser
Aquarius Services, Sleepy Hollow, NY, USA

Kit Coleman
Deep River, ON, Canada

A.N.T. INTERNATIONAL®

Advanced Nuclear Technology International
Analysvägen 5, SE-435 33 Mölnlycke
Sweden

info@antinternational.com
www.antinternational.com


Ecolabelled printed matter, 441 799

Disclaimer

The information presented in this report has been compiled and analysed by Advanced Nuclear Technology International Europe AB (ANT International®) and its subcontractors. ANT International has exercised due diligence in this work, but does not warrant the accuracy or completeness of the information. ANT International does not assume any responsibility for any consequences as a result of the use of the information for any party, except a warranty for reasonable technical skill, which is limited to the amount paid for this assignment by each ZIRAT/IZNA programme member.

Contents

1 Introduction (Peter Rudling)

The objective of the Annual Review of ZIRconium Alloy Technology (ZIRAT) and Information on Zirconium Alloys (IZNA) is to review and evaluate the latest developments in ZIRAT as they apply to nuclear fuel design and performance.

The objective is met through a review and evaluation of the most recent data on zirconium alloys and to identify the most important new information and discuss its significance in relation to fuel performance now and in the future. Included in the review are topics on materials research and development, fabrication, component design, and in-reactor performance.

Within the ZIRAT15/IZNA10 Program, the following technical meetings were covered:

- Stress Corrosion Cracking (SCC) of Nickel base alloys at Commissariat à l'Energie Atomique (CEA), Coriou effect, January 26, 2010 in Saclay, France
- Electric Power Research Institute (EPRI) 2010 Steam Generator secondary side management conference, March 2–4, 2010 in San Antonio, Texas
- 16th International Symposium on Zirconium in the Nuclear Industry, May 9–13, 2010, Chengdu, Sichuan, China
- Physor 2010 conference, May 9–14, 2010 in Pittsburgh, PA
- Jahrestagung Kerntechnik, Germany, 2010
- Contribution of Materials Investigations to Improve the Safety and Performance of Light Water Reactors (LWRs), September 26–30, 2010, Avignon, Pope's Palace, FRANCE
- 2010 LWR Fuel Performance Meeting/TopFuel/WRFPM, September 26–29, 2010, Orlando, Florida, USA
- NPC, Nuclear Plant Chemistry Conference 2010, Quebec City, Canada
- Nuclear Materials Conference, ZKM, Karlsruhe, Germany, October 4–8, 2010

The extensive, continuous flow of journal publications is being monitored by several literature searches of worldwide publications and the important papers are summarised and critically evaluated. This includes the following journals:

- Journal of Nuclear Materials
- Nuclear Engineering and Design
- Kerntechnik
- Metallurgical and Materials Transactions A
- Journal of Alloys and Compounds
- Canadian Metallurgical Quarterly
- Journal de Physique IV
- Journal of Nuclear Science and Technology
- Nuclear Science & Engineering
- Nuclear Technology

1 Introduction (Peter Rudling)

The objective of the Annual Review of ZIRconium Alloy Technology (ZIRAT) and Information on Zirconium Alloys (IZNA) is to review and evaluate the latest developments in ZIRAT as they apply to nuclear fuel design and performance.

The objective is met through a review and evaluation of the most recent data on zirconium alloys and to identify the most important new information and discuss its significance in relation to fuel performance now and in the future. Included in the review are topics on materials research and development, fabrication, component design, and in-reactor performance.

Within the ZIRAT15/IZNA10 Program, the following technical meetings were covered:

- Stress Corrosion Cracking (SCC) of Nickel base alloys at Commissariat à l'Energie Atomique (CEA), Coriou effect, January 26, 2010 in Saclay, France
- Electric Power Research Institute (EPRI) 2010 Steam Generator secondary side management conference, March 2–4, 2010 in San Antonio, Texas
- 16th International Symposium on Zirconium in the Nuclear Industry, May 9–13, 2010, Chengdu, Sichuan, China
- Physor 2010 conference, May 9–14, 2010 in Pittsburgh, PA
- Jahrestagung Kerntechnik, Germany, 2010
- Contribution of Materials Investigations to Improve the Safety and Performance of Light Water Reactors (LWRs), September 26–30, 2010, Avignon, Pope's Palace, FRANCE
- 2010 LWR Fuel Performance Meeting/TopFuel/WRFPM, September 26–29, 2010, Orlando, Florida, USA
- NPC, Nuclear Plant Chemistry Conference 2010, Quebec City, Canada
- Nuclear Materials Conference, ZKM, Karlsruhe, Germany, October 4–8, 2010

The extensive, continuous flow of journal publications is being monitored by several literature searches of worldwide publications and the important papers are summarised and critically evaluated. This includes the following journals:

- Journal of Nuclear Materials
- Nuclear Engineering and Design
- Kerntechnik
- Metallurgical and Materials Transactions A
- Journal of Alloys and Compounds
- Canadian Metallurgical Quarterly
- Journal de Physique IV
- Journal of Nuclear Science and Technology
- Nuclear Science & Engineering
- Nuclear Technology

The primary issues addressed in the review and this report is zirconium alloy research and development, fabrication, component design, ex- and in-reactor performance including:

- Regulatory bodies and utility perspectives related to fuel performance issues, fuel vendor developments of new fuel design to meet the fuel performance issues.
- Fabrication and Quality Control (QC) of zirconium manufacturing, zirconium alloy systems.
- Mechanical properties and their test methods (that are not covered in any other section in the report).
- Dimensional stability (growth and creep).
- Primary coolant chemistry and its effect on zirconium alloy component performance.
- Corrosion and hydriding mechanisms and performance of commercial alloys.
- Cladding primary failures.
- Post-failure degradation of failed fuel.
- Cladding performance in postulated accidents (Loss of Coolant Accident (LOCA), Reactivity Initiated Accident (RIA)).
- Dry storage.
- Potential Burnup (BU) limitations.
- Current uncertainties and issues needing solution are identified throughout the report.

Background data from prior periods have been included wherever needed. The data published in this Report is only from non-proprietary sources; however, their compilation, evaluations, and conclusions in the report are proprietary to ANT International and ZIRAT/IZNA members as noted on the title page.

The authors of the report are Dr. Ron Adamson, Mr. Al Strasser, Mr. Friedrich Garzarolli, Dr. Charles Patterson and, Dr. Kit Coleman and, Mr. Peter Rudling, President of ANT International.

The work reported herein will be presented in three Seminars: in Clearwater Beach, FL., USA (February 7–9, 2011), in Dubrovnik, Croatia, Europe (March 7–9, 2011) and one in Japan in 2011.

The Term of ZIRAT16/IZNA10 started on February 1, 2010 and ends on March 31, 2011.

2 BU achievements and key fuel performance issues (Alfred Strasser)

2.1 Introduction

This Section summarizes the key performance issues that could affect fuel design, fabrication or operation of the nuclear fuel in the near term or longer term. Topics covered include the fuel itself and all the Fuel Assembly (FA) components made of zirconium alloys as well as other materials. The information sources reviewed, screened and evaluated include nearly all the related publications and technical meeting presentations of the past, approximately 18 months and focuses primarily on extended BU data. The Section is intended to be a guide to significant, current issues and an alert to items that could affect fuel related operations. The extensive volume of information involved limits its presentation to the most significant features and conclusions, and the reader is urged to refer to the referenced publications or the ZIRAT or Special Topical Reports for more detailed back-up data on topics of interest.

2.2 Trends in fuel operating conditions

2.2.1 General trends

Improved fuel reliability and operating economics are the driving forces for changing operating conditions, while maintaining acceptable margins to operating and regulatory safety limits. These are incentives for significant advances in materials technology, software for modelling fuel performance, sophisticated instrumentation and methods for post-irradiation examinations. These advances have been used to increase the demands on fuel performance levels and to put pressure on the regulatory bodies to license operations to increased BU levels. The types of changes in LWR operating methods to achieve improved safety and economics have not changed in the past years and still include:

- Annual fuel cycles extended to 18 and 24 months.
- Increased discharge BUs to 58 GWD/MT batch average exposures by higher enrichments, increased number of burnable absorbers in the assemblies and in Pressurised Water Reactors (PWRs) higher Li and B levels in the coolant, or enriched B in the coolant.
- Plant power uprates that range from 5 to 20%.
- More aggressive fuel management methods with increased enrichment levels and peaking factors.
- Reduced activity transport by Zn injection into the coolant.
- Improved water chemistry controls and increased monitoring.
- Component life extension with Hydrogen Water Chemistry (HWC) and Noble Metal Chemistry (NMC) in Boiling Water Reactors (BWRs).

2.2.2 Fuel cycles

The trend for increased fuel cycle lengths has come to a near "equilibrium" in the US with PWRs operating at an average of 500 Effective Full Power Days (EFFPD) per cycle and BWRs an average of 620 EFFPD per cycle, up to a maximum of about 650 days for PWRs and 700 days for BWRs. Nearly all the US BWRs are trending toward 24 month cycles. The older, lower power density PWRs have implemented the 24 month cycles, but fuel management limitations, specifically reload batch sizes required, have limited implementation of 24 month cycles in the high power density plants. The economics of 24 month cycles tend to become plant specific since they depend on the balance of a variety of plant specific parameters. The potential economic gains for cycle extension have decreased in the US since the downtimes for reloading and maintenance procedures have been significantly reduced.

Other countries that historically have had only one peak power demand per year in the winter, compared to the two summer and winter power peaks in the US, are also trending toward longer cycles as a result of changes in economics, maintenance practices and licensing procedures. PWRs are trending toward 18-month cycles in France, the UK (Sizewell B) and Germany.

In **France,** all of the 1300 and 1450 MW_e plants and about a quarter of the 900 MWe plants are on 18-month cycles. Spent fuel is stored in their extensive pool facilities and plans are to open a high level, long lived radioactive repository by 2025.

France and Japan are both committed to **recycle plutonium** (**Pu**) in thermal reactors until fast breeders become available. The currently active recycle plan is to reprocess up to 1050 T_{HM} of spent fuel per year and reload up to 120 T_{HM} Mixed Oxide (MOX) fuel in the French PWRs. The MOX reloads are limited up to 1/3 of the core due to reactivity control considerations; however, studies are underway to implement the operation of 100% MOX cores. The amount of fuel to be reprocessed in the coming years is shown in Figure 2-1. The spent MOX fuel, shown as "Used MOX" on the Figure, is not reprocessed again and either has to be stored as a FA or separated from the FA and perhaps from some fission products, to be stored until the Pu can be used in an FBR or other power source [Arslan et al, 2010]. The separation of the useful Pu from the spent MOX will entail more waste products and its storage will have to deal with the significant decay heat and neutron radiation produced by the increased amounts of actinides. Modification of the spent fuel pools are discussed in their publication.

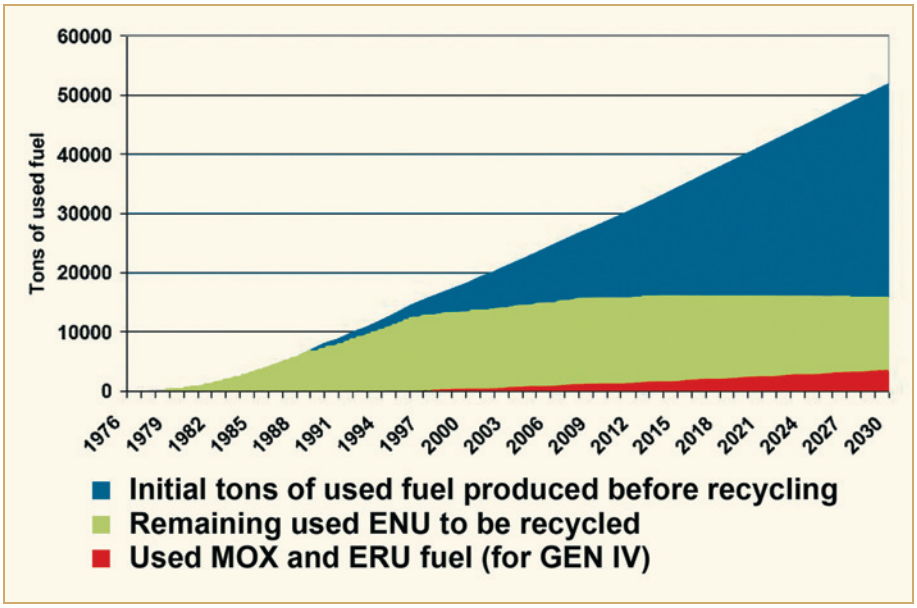

Figure 2-1: Plutonium recycling plans in France [Arslan et al, 2010].

The decreased reactivity change as a function of BU for a 100% MOX versus UO_2 core is claimed to give a more homogeneous radial and less axial peaked power distribution. This is particularly useful for increased margins under accident conditions and possibly operating margins as well. Their claim also states that "loading pattern is easily modified and burnable poisons are never necessary". Not stated is the need for increased reactivity hold-down which can not be achieved with the limited number of control rods in current and even advanced LWRs. Discussion with the author indicated that 50% enriched boron carbide control rods would be required. This type of a control rod will have a shorter life, limited by boron carbide swelling and helium release.

The development of Fast Breeder Reactors (FBRs) is continuing in France in cooperation with Japan and Russia. A prototype is planned for the 2020s and industrial scale deployment of FBRs for about 2040.

Of the 7 Reactors in **Belgium**, 4 are on 18-month cycles with the remaining 3 (Doel 1, 2, 3) on annual cycles.

Japan is planning to increase cycle lengths in several steps, first from 13 to 15 months, which does not require re-licensing, then to 18 and 24 months, which will require re-licensing. The Higashidori 1 plant of Tohoku Electric Power is the first unit to extend its cycle length and that will be to 16 months based on the 2009 change in regulations that includes a revised inspection system. The Japanese are planning to raise the current BWR 45 GWD/MT batch average BU to 50 GWD/MT. while the maximum assembly BU will remain at 55 GWD/MT for both BWRs and PWRs.

Russia has started operation of 18 month cycles at the Balaklovo units.

2.2.3 BU extension

The major incentive for extended BUs is the potentially improved fuel cycle economy. Economic analyses in past ZIRAT reports indicated that economic incentives for extending BUs beyond the 60-70 GWD/MT batch average range will disappear and that other incentives must exist in order to justify going beyond the economically optimal level. The improved economics depend in part on the decreased amount of spent FAs to be purchased and handled. This is balanced by the increased amount of uranium and enrichment services required The economics of decreased assemblies could also be impacted by the much longer cooling times required for high BU and MOX fuels in spent fuel pools prior to on-site dry storage or transport to a storage facility as noted later. The economic analyses are also dependant on the utility's accounting systems and as a result are utility and even plant specific.

The average batch BUs in US PWRs are currently in the range of 45-54 GWD/MT and in US BWRs in the range of 45-52 GWD/MT shown as a function of time in Figure 2-2 [Clifford, 2009]. The PWRs have levelled off and the BWRs are still increasing slightly, approaching the NRC regulatory limit of 62.5 GWD/MT peak rod.

Some European plants operated in the 50-58 GWD/MT batch BU range and have designed to go to 62 GWD/MT in their current cycles in both PWRs and BWRs. This is feasible, in part, due to their greater margin to regulatory BU limits. The maximum BU Lead Test Assemblies (LTAs) are in the range of 67–79 GWD/MT for both reactor types. BU ranges by countries are compared to their regulatory limits in Table 2-1.

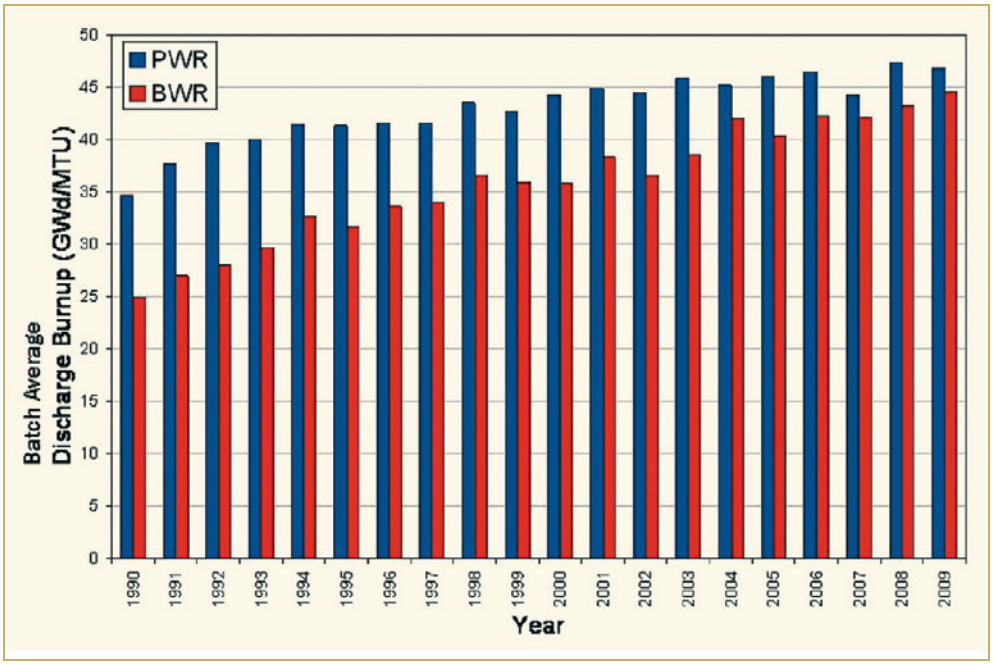

Figure 2-2: U.S. BWR & PWR fuel utilization [Clifford, 2009].

Table 2-1: Maximum BUs achieved vs. Regulatory limits (Excludes LTAs).

Country	BU (GWD/MT)				
	Batch	Assembly	Rod	Pellet	Regulatory limit
USA	54	58	62	73	62.5 peak rod
Belgium		50-55			55 UO_2 assy., 50 MOX assy.
Czech Republic	51	56	61		60 peak rod
Finland	45.6	46.5	53		45 assy
France	47	51 UO_2 42 MOX			52 assy
Germany	58	62	68		65 assy
Hungary		50	62		
Japan	50	55	62		55 UO_2 assy., 45 MOX assy.
Korean Republic	46				60 rod
Netherlands	51.5	58	64.5		60 rod
Russia	45	56	60	68	
Spain	50.4	57.4	61.7	69	
Sweden	47	57.2	63.6		60 assy., 64 rod
Switzerland	58	60	65	71	75 pellet
Taiwan					60 rod (P), 54 assy. (B)
UK	44.3	46.5	50		55 pellet
Ukraine		50			

2.3 High BU fuel performance summary

2.3.1 High BUs achieved in utility power plants

BU ranges achieved classified by vendors are summarized in Table 2-4.

Table 2-4: Maximum BU achieved by vendor fuel designs.

Vendor	Design	PWR	Design	BWR
AREVA[2] (Framatome)	Mark B-12, 15x15 Mark BW, 17x17 Mark BW, x1 (LTA) CE HTP, 14x14 FOCUS HTP DxD4, HTP M5 DXELS 0.8	50 assy 52 assy, 58 rod 68 assy., 72 rod 48 assy. 58 batch, 60 assy. 57-60 batch, 58-60 assy	ATRIUM 10XM ATRIUM 10XL ATRIUM 10XP	53 batch, 57 assy., 64 rod 30 rod 54 batch, 60 assy., 62 rod
Global Nuclear Fuel (GNF)			GE[3]12 GE14 GNF2	50 batch, 68 assy. 52 batch, 72 assy. 10 batch, 43 assy.
Westinghouse (W)	ZIRLO[4] { OFA. 17x17 Std, 17x17 V, 14x14 opt. ZIRLO, NGF (LTA) RFA[5]-2	56 batch, 68 assy. 48 assy. 52 assy. 63 assy. 49 batch, 55 assy., 60 rods 68 assy., (LTA)	Optima 2	57 batch, 60 assy.
TVEL	TVA[6], TVS TVS-2	58 assy. 48 assy.		

The ***highest BU levels in PWRs*** have been implemented in the US, Germany, Netherlands, Russia and Switzerland. The batch averages range between 47 and 60 GWD/MT with plans to go to 62 GWD/MT in Germany. The peak assemblies range between 48 and 72 GWD/MT and the peak rods between 53 and 106 GWD/MT BU.

The increase in batch average BU levels in the US plants as a function of years is shown on Figure 2-2. The BU levels in PWRs have reached their maximum level permitted by the 62 GWD/MT max. rod exposure established by the NRC, until more data become available to justify increased regulatory BU limits. Peak assembly average BUs in both the US PWRs and BWRs are in the range of 58 to 68 GWD/MT. BUs above this level are in German, Russian and Swiss plants.

MOX assemblies have reached peak assembly average BUs of 62 GWD/MT (75 GWD/MT peak rod) in PWRs and 58 GWD/MT in BWRs in European plants.

The current examinations of US rods from LTAs above the 62 GWD/MT limit are intended to justify the increase of the current limit to 70 or 75 GWD/MT. While the French PWRs are limited to 52 GWD/MT assembly average BU by their regulatory body, the current goal of the industry is to increase the limit to 70 GWD/MT. Similarly, the Japanese utilities, while they have relatively conservative current BU levels, have an irradiation program to raise this to 90-100 GWD/MT rod BU. This situation has not changed in the past years.

[2] French Equipment Manufacturer
[3] General Electric
[4] ZIRconium Low Oxidation
[5] Robust Fuel Assembly
[6] Tennessee Valley Authority

2.3 High BU fuel performance summary

2.3.1 High BUs achieved in utility power plants

BU ranges achieved classified by vendors are summarized in Table 2-4.

Table 2-4: Maximum BU achieved by vendor fuel designs.

Vendor	Design	PWR	Design	BWR
AREVA[2] (Framatome)	Mark B-12, 15x15 Mark BW, 17x17 Mark BW, x1 (LTA) CE HTP, 14x14 FOCUS HTP DxD4, HTP M5 DXELS 0.8	50 assy 52 assy, 58 rod 68 assy., 72 rod 48 assy. 58 batch, 60 assy. 57-60 batch, 58-60 assy	ATRIUM 10XM ATRIUM 10XL ATRIUM 10XP	53 batch, 57 assy., 64 rod 30 rod 54 batch, 60 assy., 62 rod
Global Nuclear Fuel (GNF)			GE[3]12 GE14 GNF2	50 batch, 68 assy. 52 batch, 72 assy. 10 batch, 43 assy.
Westinghouse (W)	ZIRLO[4] { OFA. 17x17 Std, 17x17 V, 14x14 opt. ZIRLO, NGF (LTA) RFA[5]-2	56 batch, 68 assy. 48 assy. 52 assy. 63 assy. 49 batch, 55 assy., 60 rods 68 assy., (LTA)	Optima 2	57 batch, 60 assy.
TVEL	TVA[6], TVS TVS-2	58 assy. 48 assy.		

The ***highest BU levels in PWRs*** have been implemented in the US, Germany, Netherlands, Russia and Switzerland. The batch averages range between 47 and 60 GWD/MT with plans to go to 62 GWD/MT in Germany. The peak assemblies range between 48 and 72 GWD/MT and the peak rods between 53 and 106 GWD/MT BU.

The increase in batch average BU levels in the US plants as a function of years is shown on Figure 2-2. The BU levels in PWRs have reached their maximum level permitted by the 62 GWD/MT max. rod exposure established by the NRC, until more data become available to justify increased regulatory BU limits. Peak assembly average BUs in both the US PWRs and BWRs are in the range of 58 to 68 GWD/MT. BUs above this level are in German, Russian and Swiss plants.

MOX assemblies have reached peak assembly average BUs of 62 GWD/MT (75 GWD/MT peak rod) in PWRs and 58 GWD/MT in BWRs in European plants.

The current examinations of US rods from LTAs above the 62 GWD/MT limit are intended to justify the increase of the current limit to 70 or 75 GWD/MT. While the French PWRs are limited to 52 GWD/MT assembly average BU by their regulatory body, the current goal of the industry is to increase the limit to 70 GWD/MT. Similarly, the Japanese utilities, while they have relatively conservative current BU levels, have an irradiation program to raise this to 90-100 GWD/MT rod BU. This situation has not changed in the past years.

[2] French Equipment Manufacturer
[3] General Electric
[4] ZIRconium Low Oxidation
[5] Robust Fuel Assembly
[6] Tennessee Valley Authority

The lead test assemblies (LTAs) are usually exempt from regulatory limits and their highest peak rod BUs achieved in the past years have been in GWD/MT: 72 (US, Russia), 80 (France), 75 (Japan), 106 (Switzerland).

The peak BUs in GWD/MT achieved by the current PWR cladding materials have been:

	Batch	Assembly	Rod
ZIRLO, standard	55	58	75
ZIRLO, optimized		63	65
AXIOM (1,2,4,5)		65-72	>75 (LTA)
AXIOM (5A)			58-69
M5	54	68	80
E-110		62	73
Duplex , various	58	62	68
PCA2b	49	55	58
M-MDA[7]		68	73
J-Alloy			50

The ***highest BUs in BWRs*** are in the US, Germany, Spain and Switzerland. The batch averages range between 43 and 57 GWD/MT, peak assemblies between 57 and 75 GWD/MT and the peak rods between 60 and 82 GWD/MT. The BU levels in BWRs are catching up to those of the PWRs in the US, as shown in Figure 2-2, probably because both reactor types are reaching the current NRC BU limitation. Irradiation results of a variety of BWR vendor fuel designs in KernKraftwerk Gundremmingen (KKG) and KernKraftwerk Leibstadt (KKL) to extended BUs are of significant interest in this regard when published.

The highest peak rod BUs achieved in LTAs have been in GWD/MT: 63 (Spain), 65 (US), 72 (Japan), 73 (Switzerland), 75 (Germany).

The peak BUs achieved by the current BWR cladding materials have been:

Zircaloy-2 (GWD/MT)	:	49 batch, 71 assembly, 78 rod,
LK3 (GWD/MT)	:	47 batch, 53 assembly, 81 rod.

The assembly and rod BUs listed above were achieved without failures; however, FAs and materials do not have a perfect performance record up to these BUs levels and the related problems are summarized in Section 2.4 and discussed in detail in subsequent Sections of this Report.

2.3.2 High BU UO_2 and MOX fuel examination results

2.3.2.1 High Burnup Structure (HBS) in UO_2 and MOX

A rim of HBS is formed on the pellet Outer Diameter (OD) initiated in the range of 50-60 GWD/MT pellet average BUs, the product of the transformation, or recrystallization, of the as fabricated grains into submicron grain sizes (Figure 2-3). A plot of over 200 HBS width data points as a function of up to 105 GWD/MT BU showed considerable scatter, as reported in ZIRAT14 (Figure 2-4). A recent French study analyzed all their data as well as that from outside sources to identify the parameters, which govern the formation of the HBS [Lemoine et al, 2010]. The causes of the scatter were attributed to:

- Various fuel designs, (enrichment, Pu content),
- different irradiation conditions, (neutron flux spectrum, relative Pu buildup, local fission rate and local BU),
- different definitions of the HBS,
- different HBS width measurement methods.

[7] Modified Mitsubishi Developed Alloy

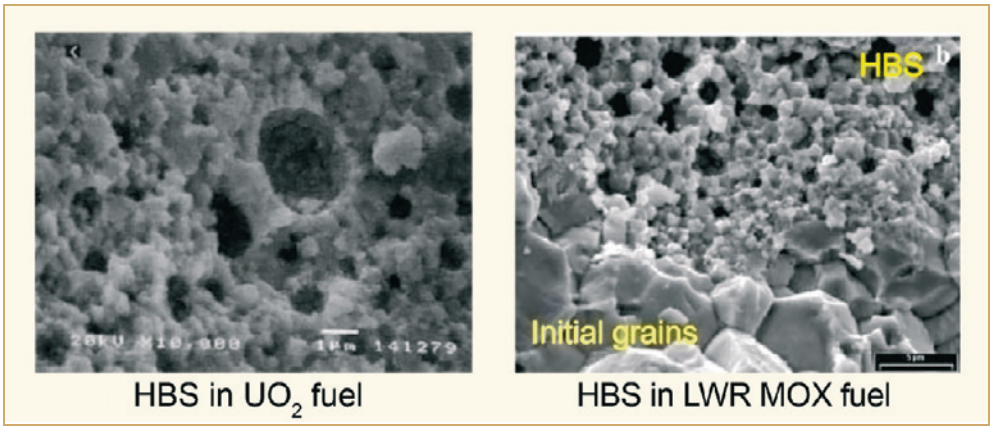

Figure 2-3: HBS grain structure [Lemoine et al, 2010].

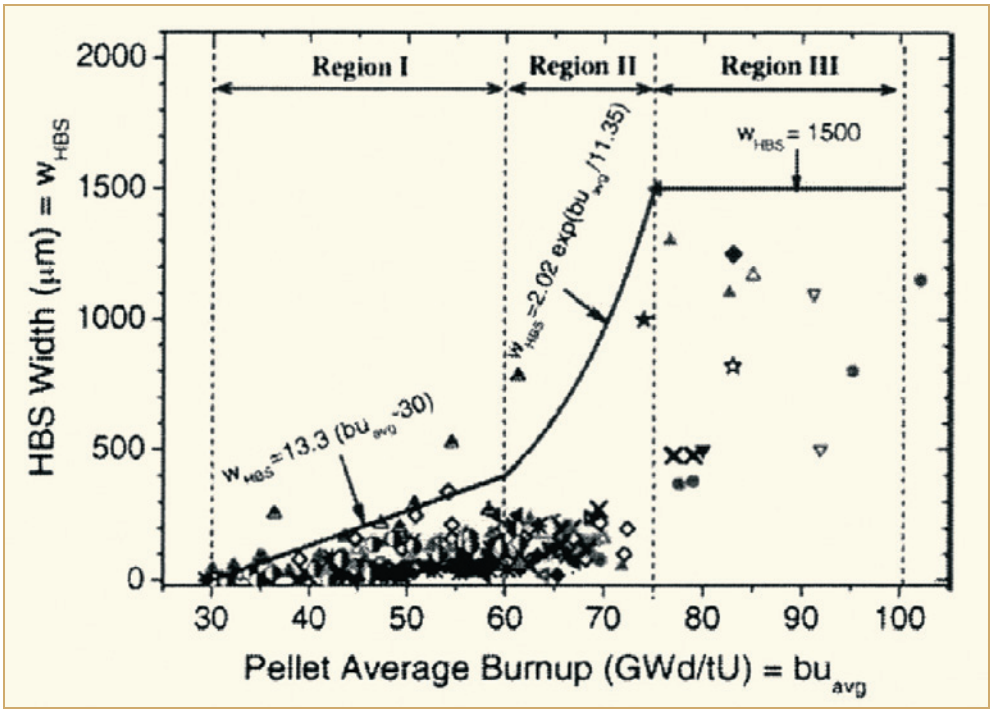

Figure 2-4: A conservative HBS width in LWR UO_2 fuel pellet as a function of pellet average BU in the three regions [Koo et al, 2009a].

As noted above, the HBS formation is dependant on the local BU as well as the average BU of the pellet. Width variations of as much as 30-130μ were measured on the periphery of PWR fuels irradiated to 63 GWD/MT. Azimuthal variations up to a factor of 2 were found on rods at this high exposure level. The azimuthal heterogeneity was more pronounced for rods in front of water holes in the assembly. The variations in HBS widths appear to be due to variations in local BU, caused by the variation in local neutron flux spectrum, which leads to differences in local Pu buildup, local fission density, radial power profile, local fission rate and finally local BU.

3 Microstructure (Ron Adamson)

3.1 Introduction: Crystallography and texture

At temperatures below about 825 °C zirconium alloys have the hexagonal-close-packed (hcp) structure. Important planes in that structure are shown in Figure 3-1 [Tenckhoff, 2005]: basal plane, prism plane and pyramidal plane. The unit cell is marked by the heavy lines in Figure 3-1.

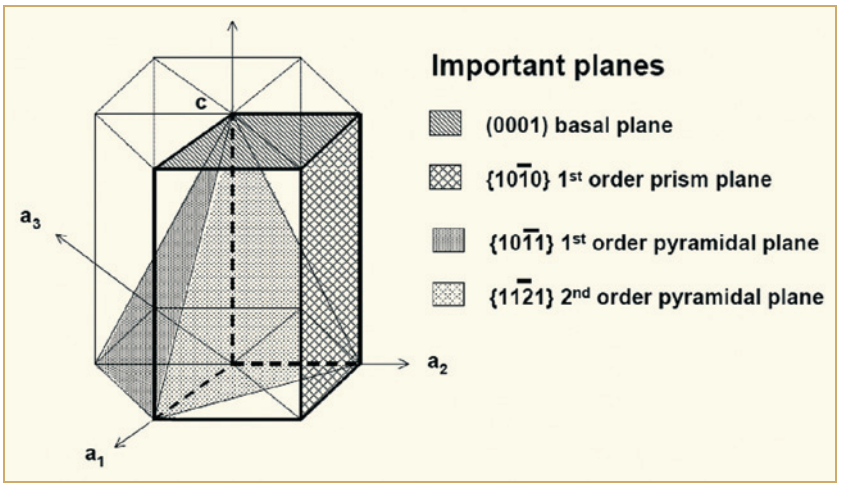

Figure 3-1: Crystallographic characterizations of the hcp elementary cell [Tenckhoff, 2005].

In the hexagonal close-packed crystal structure, as for zirconium alloys, the Miller-Bravais system is used to identify planes and directions. The indices are based on four axes: the three axes a_1, a_2, a_3, are 120 °C apart in the basal plane, and the vertical c axis is normal to the basal plane, as shown in Figure 3-1, and the indices are given as (hkil). For clarity, (hkil) indicates a specific plane, while {hkil} indicates a family of planes, identical in geometry relative to the lattice, but identified specifically depending on the choice of axis origin. For instance $(10\bar{1}0)$, $(01\bar{1}0)$ and $(1\bar{1}00)$ are all prism planes of the $\{10\bar{1}0\}$ family. The indices indicate the reciprocal of intercept of the plane on the four crystal axes. Example: a $(10\bar{1}0)$ plane intercepts the a_1 axis at 1 unit, the a_2 axis at infinity (∞), the a_3 axis at -1 unit, and the c axis at infinity. It is noted that i= -(h+k). The indice l indicates the reciprocal of where the plane of interest intercepts the c-axis. For prism planes this is at ∞, so $l=\frac{1}{\infty}=0$ indicates the plane is perpendicular to the basal plane, and when l≠0, the plane is inclined at some angle to the basal plane. The basal plane itself is therefore designated as (0001), but could be (0002), and pyramidal planes (see Figure 3-1) are $\{10\bar{1}1\}$ and $\{11\bar{2}1\}$.

Directions in the HCP system are given as [hkil], but reciprocals are not used for directions. Families of directions are given as <hkil>. Often directions are given in terms of the a or c axes, so that "<c> component" or "$\bar{c}$-component" dislocations have Burgers vectors with a strong component in the c-direction [0001] in it. Similar terminology applies to <a> component or $\bar{c}$-component dislocations.

Texture of commonly described by pole figures obtained by X-ray diffraction, by Kearns f-parameter numbers calculated from pole figures, and, less commonly, by a mechanical measure of Contractile Strain Ratio (CSR). Figure 3-2 gives a direct pole figure for a typical fuel cladding tube. What is shown is a 2-dimensional (stereographic) projection of a 3-dimensional (spherical) distribution of the normals to the basal planes (pole) of a large number of grains in the cladding. [Note: if the average grain size is greater than about 40 μm (ASTM 36) the measurements become unreliable [Lewis et al, 1982]. The pole figure is defined by three directions in the tubing: LD (axial), TD (circumferential) and ND (radial or through-thickness). The numbered contours give the times-random intensity of the basal pole in the given direction. In this specific case the value is highest along the TD direction (value 6-7) and quite low in the LD direction. In stereographic projections there is a 90° angle between the ND and TD or LD directions, and for Figure 3-2 the maximum intensity of basal plane poles is about 30° from the radial direction in the tube. This is seen more easily in Figure 3-3 where the basal pole intensity in the TD-ND plane is plotted as a function of angle.

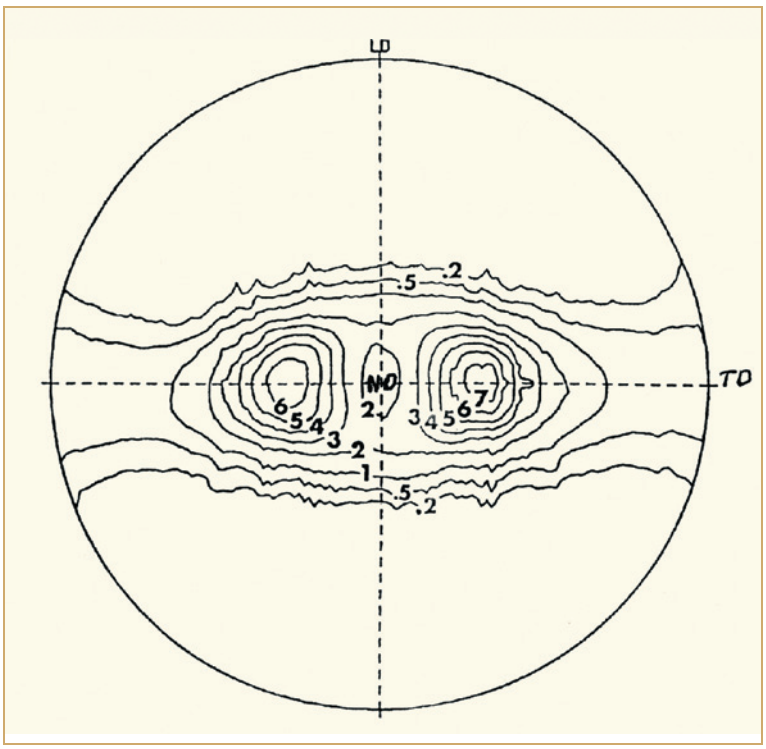

Figure 3-2: Typical texture of CW Zircaloy cladding tube. (0002) direct pole figure [Lewis et al, 1982].

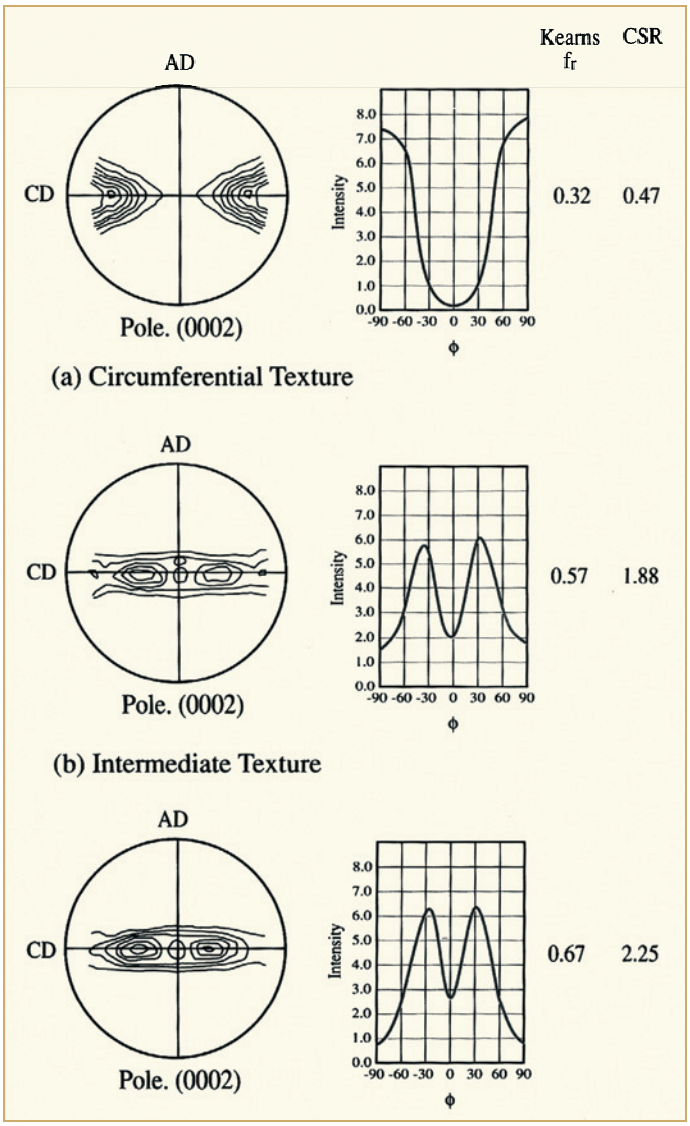

Figure 3-3: Crystal texture represented by (0002) pole figure, intensity plot, Kearns texture parameter and CSR [Schemel, 1989].

To obtain a more complete description, pole figures of other planes are generally obtained. Figure 3-4 gives the companion $(10\bar{1}0)$ prism pole distribution for the Figure 3-2 tube. It is seen for this ~70% cold-worked tube the prism poles are strongly aligned in the LD direction. This is common for cold-worked tubing.

4 Mechanical properties

4.1 Introduction: Deformation of irradiated zirconium alloys (Ron Adamson)

As described in the previous section, in the temperature range 20-350 ºC deformation in zirconium alloys occurs predominately by relatively uniform motion of dislocations on prism $\{10\bar{1}0\}$ planes. For irradiated materials, the deformation is quite different, with the deformation being localized in narrow bands (swaths) called dislocation channels, which are cleared of irradiation damage. The result is dramatically illustrated in Figure 4-1 for irradiated and deformed copper single crystals. In this study the deformed specimen is plated with copper to preserve the surface and then sliced for TEM exam in a way to reveal the expected channelling plane. The mottled background is the irradiation damage (small dislocation loops, as in zirconium alloys) and the white swaths are channels created by avalanches of dislocations along the {111} slip planes in Face Centred Cubic (FCC) copper. Massive slip steps at the surface are indicative of local shear strain is in excess of 100%.

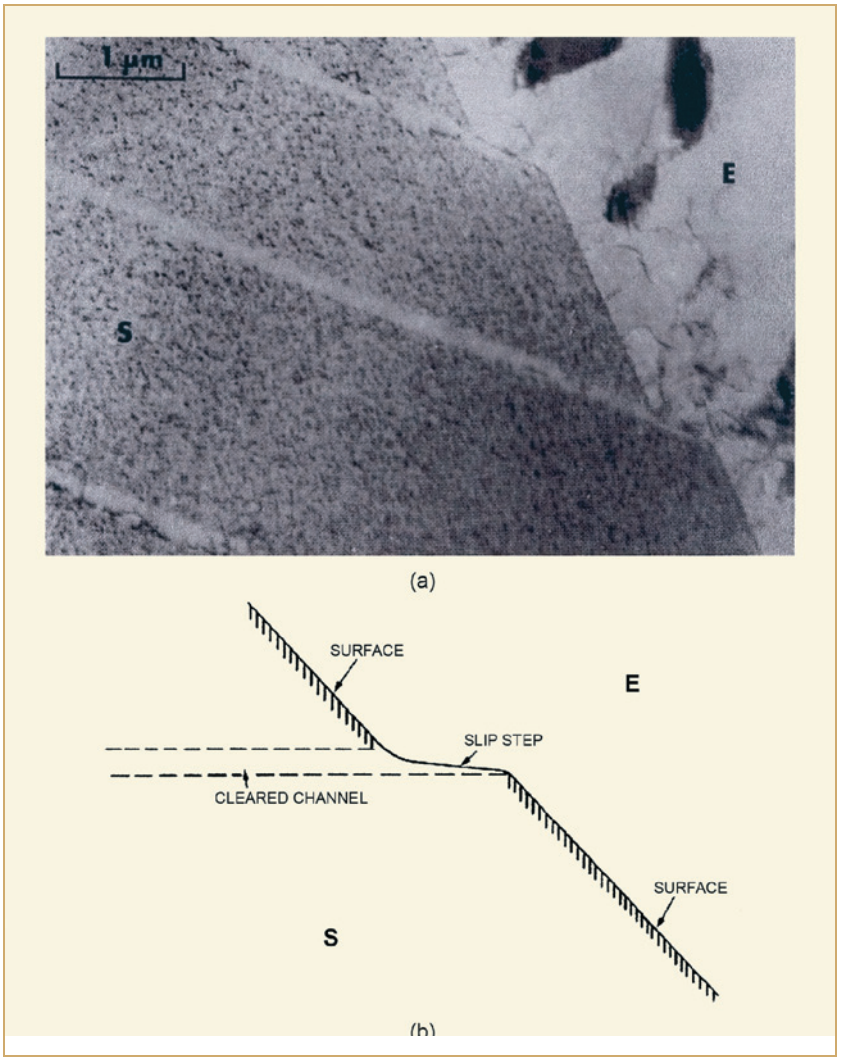

Figure 4-1: Correlation of dislocations and surface slip steps on copper single crystal irradiated with neutrons and deformed in tension [Sharp, 1972].

As nicely summarized in [Rosenbaum, 1975], [Wechsler, 1973] and [Schmidt, 1970], early observations of channels in Body Centred Cubic (BCC) and face centred cubic (FCC) materials indicated that channelling occurred on planes which were the normal deformation planes for non-irradiated material. Good examples are given for copper [Sharp, 1967] and [Adamson, 1968], niobium [Tucker & Ohr, 1967] and molybdenum [Brimhall, 1965]. The known increase in strength of irradiated as compared to unirradiated material is attributed to interaction of mobile dislocations with irradiation-produced dislocation loops, which increases the stress required to maintain a given imposed strain rate. That general process is illustrated in Figure 4-2 for irradiated copper. As the dislocation attempts to move to the right in the figure, it is impeded, as shown by the bowed dislocation segments. When the applied stress becomes sufficiently high, the moving dislocation can interact with the irradiation-damage loops, either moving it out of the slip plane or absorbing it. This begins the avalanche process by which the slip plane is cleared of defects, allowing an easy path for dislocation motion. The channel widens until work hardening occurs within a single channel sufficient to impede further dislocation motion there. This process is beyond the scope of this introduction, but some of the basics for non-Zr are given in [Makin, 1964], [Foreman & Sharp, 1969] and [Foreman, 1968]. More information for zirconium alloys is presented below.

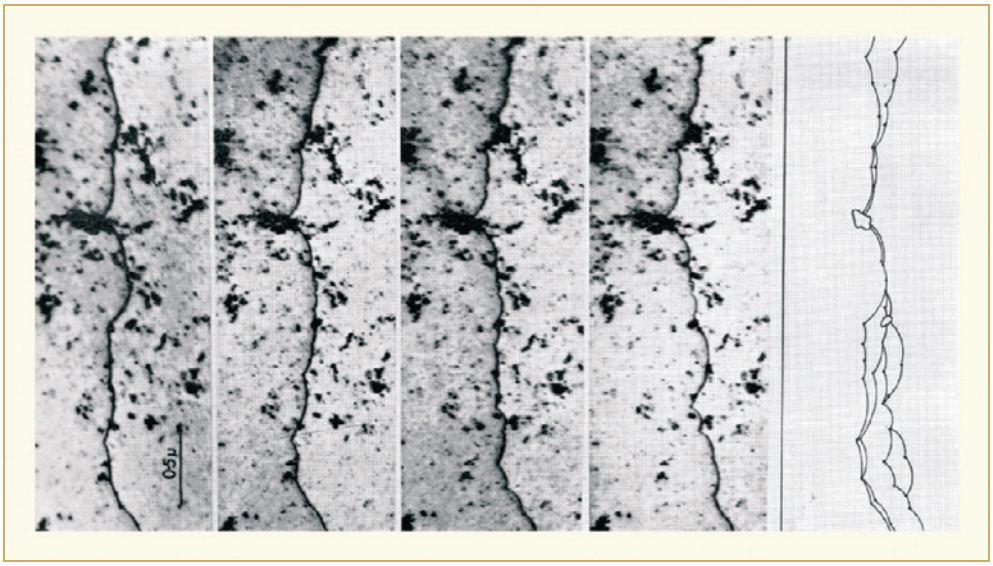

Figure 4-2: Interaction of a dislocation-under-stress with irradiation-induced defects. The dislocation is moving “to the right” [Barnes, 1965].

For irradiated zirconium alloys, because normal slip systems are limited and the crystal structure is highly textured in fabricated components and even in single crystals, deformation is more restricted. It would be expected that dislocation channelling would occur on the prism planes, as is normal for unirradiated material, but this is not necessarily the case.

To facilitate mechanical modelling of deformation in zirconium alloys, it is important to know the details of strain localization, including the crystallography of the deformations. Only then can a reliable micro-mechanical model be developed.

Factors, which appear to influence the choice of channelling plane include:

1) Testing direction relative to the existing texture,
2) testing temperature,
3) oxygen content in the alloy,
4) fluence magnitude (irradiation defect density),
5) irradiation temperature.

Factor 1 is dominated by what is known as Schmidt's Law, which determines the resolved shear stress on a particular deformation plane. The resolved shear stress τ_R is given as:

Eq. 4-1: $$\tau_R = \frac{F}{A} (\cos \phi \cos \lambda)$$

where as shown in Figure 4-3

F = applied force
A = area normal to F
ϕ = angle between the force direction and normal to the slip plane
λ = angle between the force direction and the slip direction.

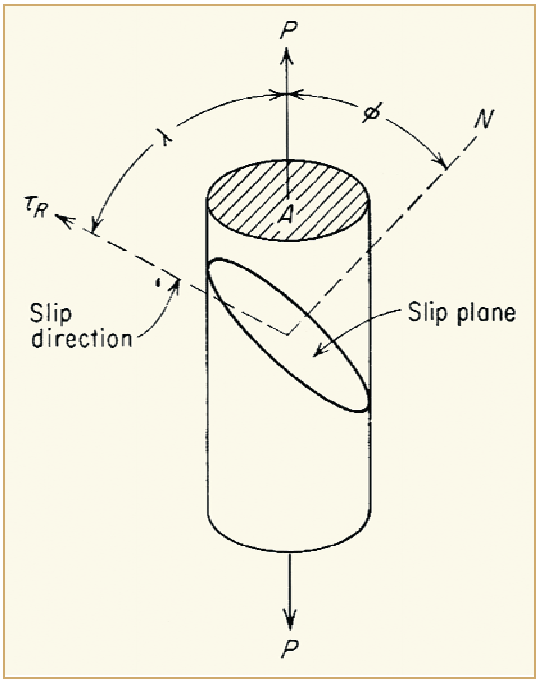

Figure 4-3: Diagram for calculating the Critical Resolved Shear Stress (CRSS) [Dieter, 1961].

For example, Figure 4-4 depicts the extreme texture (achieved in a cross-rolled plate) where all the basal poles lie in the rolling plane of a sheet, giving f_N=1, f_t=0, f_l=0. If a force F is applied in the rolling direction along the slip direction $[\bar{2}110]$ then for the basal plane B, prism plane P_1 and prism plane P_2,

τ_B = cos90 cos180 = 0 x 1 = 0
τ_{P_2} = cos30 cos60 = .87 x .50 = .44
τ_{P_1} = cos90 cos180 = 0 x 1 = 0

Of perhaps more interest is the creation of a composite structure by the addition of carbon nanotubes to the alloys. No microstructure or fabrication details (except to mention solid-phase powders) are provided. Increases in the strength parameters of E110 by 20-40% are reported, with a loss of ductility of less than 5%. Increases in the axial creep strength of 3-45 % is also reported. Improvements in the deleterious effects of hydrogen are also indicated. (Carbon nanotubes for other applications have been shown to irreversibly absorb (surface absorption) hydrogen). Data (Table 4-13), is given illustrating that Carbon Micro tube additions (CM) dictate that hydride orientation is maintained in the tubing circumferential direction independent of the tubing reduction schedule (denoted by an undefined "Q") whereas for E110 or E635 the value of "Q" is restricted to be above 1.

The practicality or the interactions with irradiation effects remains unproven.

Table 4-13: Hydride orientations as affected by fabrication processes [Ivanova et al, 2010].

Dependence of orientation factor of hydrides on cold rolling process parameters		
Cold rolling process parameter Q	Orientation factor of hydrides F_a	
	E110 alloy tube	CM tube
0.54	0.6	0.1
0.75	0.5	0.1
0.87	0.4	0.1
1.6	0.4	0.1
2.8	0.4	0.1
3.8	0.2-0.3	0.1

4.3 An introduction to Delayed Hydride Cracking (DHC) in zirconium alloys (Kit Coleman)

4.3.1 Abstract

Hydrogen, in the form of hydrides, has been responsible for several failures in components made from zirconium alloys in both nuclear and chemical plants. This paper describes the mechanism of these failures caused by a time-dependent phenomenon called DHC. The most notable failures were in pressure tubes made from Zr-2.5Nb, but cracking in Zircaloy fuel cladding may also be caused by this mechanism. In DHC, hydrogen moves but hydrides crack. The requirements for the presence of hydrides are described and the range of conditions of loading and temperature history that induce cracking are reviewed. A method for safeguarding and assessing components by answering seven questions is outlined.

4.3.2 Introduction

When present in structural components, hydrides may be responsible for loss in integrity because they are brittle. In the Periodic Table the affected metals of most importance are those in Group 4 – titanium, zirconium and hafnium – and Group 5 – vanadium, niobium and tantalum [Coleman, 2003]. The damaging effect of hydrides may take the form of a reduction in short-term crack growth resistance and tensile ductility or in the form of time dependent processes. Hydrogen diffuses up stress gradients, down temperature gradients, up or down alloy solute concentration gradients and down hydrogen concentration gradients. This movement may lead to time dependent failure when the solubility limit is exceeded and hydrides form. In a water-cooled nuclear reactor, hydrogen is absorbed by a component during service as a consequence of corrosion. The hydrogen movement and increase in concentration necessitate continuous vigilance during the life of the component to ensure it performs as designed.

Time dependent cracking associated with hydrogen and hydrides was recognized as an important failure mechanism in titanium alloys in the 1950s [Kessler et al, 1955]. This failure mechanism, called **S**ustained **L**oad **C**racking (SLC), was characterized by a cracking rate, V that was highly dependent on temperature but had low dependence on load once a threshold value was exceeded. Although it turns out that zirconium alloys are much more sensitive to time-dependent hydride cracking than titanium alloys, the phenomenon became more than a laboratory curiosity in zirconium alloys only in the mid-1970s. Early indications were that zirconium alloys had high tolerance to such time dependent fracture. In tests at room temperature, notched tensile specimens of Zr-1.25Al-1Sn-1Mo in the annealed condition and containing 500 ppm hydrogen showed the characteristic behaviour of increase in time to failure as the applied stress was reduced (Figure 4-1). Specimens failed in 30 hours at about half the notched UTS, in 200 hours at 0.3 of the notched UTS, and did not fail in over 1100 hours at 0.2 of the notched UTS [Weinstein & Holtz, 1964]. Quenched and aged Zr-2.5Nb gave a slight indication of delayed failure within the limits of the test time (1000 hours), while annealed or cold-worked Zircaloy (Zr-1.5 wt.% Sn) was completely resistant. Östberg [Östberg, 1964] found some suggestion of delayed failure in Zircaloy containing 10 ppm hydrogen in tests at 100 °C.

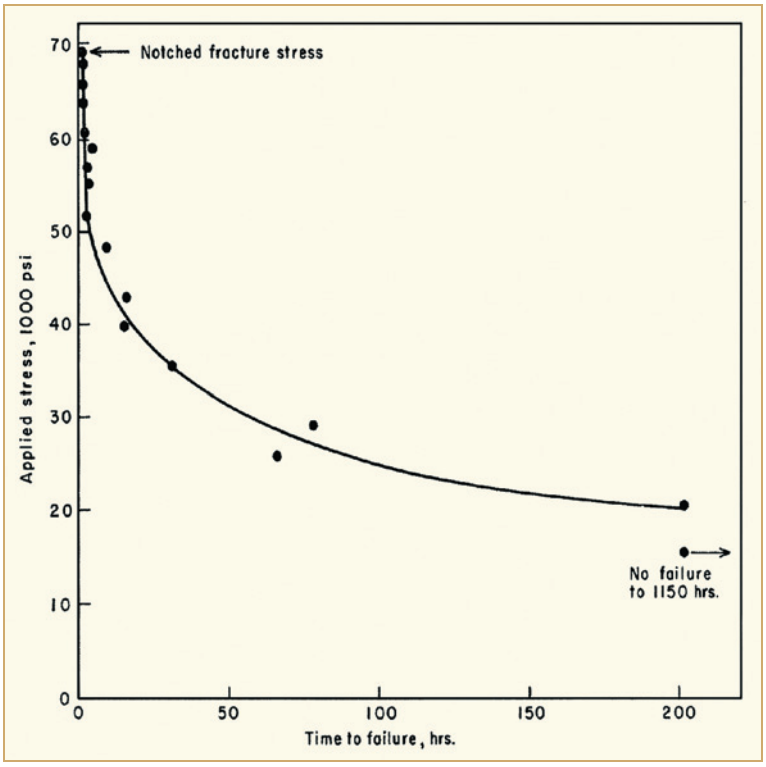

Figure 4-47: Delayed failure curve at room temperature of notched Zr-1.25Al-1Sn-1Mo specimens containing 500 ppm hydrogen [Weinstein & Holtz, 1964].

The cracking of Zr-2.5Nb pressure tubes in CANDU and Reaktor Bolshoi Mozhnosti Kanalov (in English Large Boiling Water Channel type reactor) (RBMK) reactors abruptly changed the perception on time dependent failure and generated much research into the phenomenon. The time dependent cracking in zirconium alloys has had several names but the accepted one is DHC[13]. The phenomenology is similar to that of SLC in titanium alloys. In this paper the experience with this type of cracking is outlined, the basic mechanism and phenomenology are described along with a brief presentation on the current controversy on models of crack growth rate, then the questions for assessment of structural integrity are posed.

4.3.3 Component failure by DHC

4.3.3.1 Experience with pressure tubes

4.3.3.1.1 Pickering 3 and 4: 1974 and 1975

High residual stresses were responsible for the cracking in Zr-2.5Nb pressure tubes after two to three years of operation. In CANDU reactors, the pressure tubes are 4 mm thick, have an inside diameter of 103 mm and a length of 6 m. Each end is placed inside a thick-walled tube of 403 SS containing three internal, circumferential grooves – the end-fitting – and the pressure tube is internally rolled to make a seal at the grooves; this configuration is called a rolled-joint. If the rolls are advanced too far – called over-rolling or over-extension – part of the pressure tube is deformed without support from the SS and large residual tensile hoop stresses arise locally (Figure 4-48). A second factor is the clearance between the pressure tube and the end-fitting; the larger the clearance, the higher the residual stress. A combination of over-rolling and high clearance could produce residual stresses well over 500 MPa. Consequently, cracks may initiate. (Note that the hoop stress from the operating pressure is at least three times lower than these residual stresses.) When the cracks penetrated the pressure tube wall in 1974 (Pickering 3) and 1975 (Pickering 4), heat-transport water leaked and was detected in the gas annulus between the pressure and calandria tubes, and the reactor was shutdown. This behaviour is an example of an approach to Leak-Before-Break (LBB): detect and identify a growing and leaking but stable crack before it reaches its Critical Crack Length (CCL) and becomes unstable. Once the leaking tubes were identified, they were removed and replaced. Out of 780 tubes, eighteen in Pickering 3 and two in Pickering 4 leaked [Ross-Ross et al, 1976], [Jackman & Dunn, 1976] and [Perryman, 1978]. Only one more leaking crack was detected after the initial set of failures.

[13] The other names that have been used in the technical literature are: delayed failure hydrogen embrittlement, delayed hydrogen embrittlement, delayed hydrogen cracking, hydrogen assisted subcritical crack growth, hydrogen-induced delayed cracking, and hydride-induced crack growth.

5 Dimensional stability (Ron Adamson)

A limited amount of information was published on this topic during the last 18 months. Dimensional stability will be covered in ZIRAT16 (next year).

6 Corrosion and hydriding (Friedrich Garzarolli)

6.1 Out of reactor corrosion and hydriding

6.1.1 General

Zirconium and its alloys are highly reactive metals and in oxygen containing atmospheres always have at least a thin oxide film on their surfaces. At intermediate temperatures (> ~200 °C) the air-formed oxide will grow by oxygen diffusion through the air-formed oxide forming a layer of ZrO_2 at the oxide metal interface.

If the oxidation environment is water the water molecules are dissociated at the oxide/environment interface by the electrons from the oxidation process at the metal/oxide interface. These oxygen ions fill up oxygen ion vacancies at the oxide/environment interface and then migrate to the metal/oxide interface. The hydrogen atoms resulting from the reduction of the protons (from the water molecule) at the oxide/environment interface may either recombine and form hydrogen molecules, which will go into the water or as hydrogen atoms go into the Zr alloy metal. The fraction of hydrogen produced by the corrosion reaction that goes into the metal is usually called the hydrogen pickup fraction (HPUF). The corrosion behaviour of the Zr alloy depends on:

- The temperature (usually tests at ≥250 to ≤550 °C, are applied for out-reactor studies).
- The environment (which can be oxygen, CO_2, pressurized water or steam or SuperCritical Water (SCW). For tests in water and steam the oxygen content, hydrogen content and potential additions such as boric acid, LiOH, H_2S, etc. are important).
- The alloying (Sn, Nb, Fe, Cr, V, etc.) and impurity (C, Si, etc.) content of the material.
- The material condition (governed by process steps, the quenching rates (distribution of the alloying elements), the intermediate annealing temperatures, the final CW and the final annealing (size and distribution of second phase precipitates as well as dislocation density).

6.1.2 Effect of corrosion environment on corrosion behaviour in autoclaves

The corrosion tests of Zr-alloys for reactor fuel are usually performed either in degassed pressurized water at ≤360 °C or in degassed 400-550 °C steam either in static autoclave or in refreshed systems.

There are two different types of static autoclaves, as follows:

- Small tubular autoclaves fabricated from Zircaloy tubing or SS tubings (mini-autoclaves) have been used. In mini-autoclave tests a few corrosion specimens is loaded into the autoclave, after which it is half filled with more or less air saturated water, potentially containing additives. After this the mini-autoclave is sealed. The mini-autoclaves are opened periodically to measure the WG of individual specimens after rinsing and drying the speciments. The mini-autoclave solution is replaced with fresh solution after each inspection.

- A 5-10 litre SS autoclave fitted with devices for measurement and control of pressure and temperature, safety devices, and venting valves. For such tests deionized water is used, eventually certain species such as LiOH or H_3BO_3 are added. To eliminate the oxygen from the water different techniques have been applied for such static tests by:

  – Filling the clean and thoroughly rinsed autoclave with deionized water, heating to about 95 °C and venting it for at least 6 min.

  – Filling the autoclave with about 10% more than needed deionized water, sealing it and heat it up to about 150 °C, open the vent valve for a sufficient time to degas the water, but keeping the specimens covered with water (in case of steam tests degassing is done (in several steps) to adjust to the desired pressure).

  – Filling the autoclave with deionized water and purging it with Ar gas, evacuating and backfilling with Ar to a gage pressure of 3.5 to 5 bar several times. Potentially a hydrogen pressure of about ≥0.25 bar is also applied sometimes in addition with boric acid and lithium hydroxide additions to get a typical PWR water chemistry in the autoclave.

    Furthermore, often the autoclave load with specimens is restricted according to ASTM Standard G 2M– 88. This standard limits the total surface area of specimens loaded in a static autoclave to < 0.1 m^2/litre.

For tests in a refreshed system the water is usually supplied from a water tank containing high purity water, which usually is degassed. Deoxygenation is mostly done by N_2 gas, which is bubbled from the bottom of the tank. In other cases hydrazine is added to the water tank. Here also boric acid and lithium hydroxide or other species may be added. The water is pumped to a pre-heater. Potentially hydrogen is injected in this line. From the pre-heater, the water or steam passes into the autoclave. The water/steam pressure in the autoclave is regulated via a condenser and a pressure regulating valve.

Most of the autoclave tests have been performed in degassed water or steam without further additions. However, some tests were desired to be give corrosion information for water conditions more closely to the reactor water chemistry. In such cases oxygen (e.g. 200-400 ppb) or hydrogen peroxide is added to simulate the in-BWR water chemistry more closely or hydrogen or hydrogen plus boric acid plus lithium hydroxide is added to simulate the in-PWR water chemistry. For evaluation of the corrosion effect of LiOH enrichments in ZrO_2 and the corrosion effect of other impurities and CRUD deposits tests have been made with varying concentrations of LiOH, H_3BO_4, F, H_2S, H_2SO_4, etc. or larger amounts of different Fe-, Ni-, and Cr-oxides. In cases of mini autoclaves, were an evacuation treatment is not possible often hydrazine is added to eliminate the oxygen of the water during the heating up phase.

For Zr-alloys, there are different corrosion phenomena of interest, such as uniform corrosion for PWR und nodular corrosion for BWR. Different test conditions have to be applied depending on the kind of corrosion to be studied.

- Water and steam tests with temperatures up to 450 °C are applied to study the uniform corrosion behaviour and

- high pressure steam tests, at ≥100 bar and ≥460 °C to 520 °C for estimation of the material tendency to nodular corrosion.

The corrosion behaviour measured in such tests depends on the environment.

- Variation of the gas content have only a moderate effect on uniform of normal Zircaloy-4 in pressurized water (Figure 6-1), whereas a dramatic effect of oxygen additions have been seen for Zr-Nb alloys.

- A fully removal of any oxygen and hydrogen additions can cause a significant change of the corrosion rate, as can be seen from Figure 6-2. In an environment without any hydrogen additions and probably not perfect O_2 removal the corrosion rate of Zry-4 appears to depend primarily on yield strength, but in an O_2 free environment with H_2 addition the SPP size becomes the main parameter impacting the corrosion behaviour.

- Additions of oxygen or H_2O_2 in oxygen free pressurized water and steam affect the corrosion rate of Zircaloy coupons with very fine SPP (Figure 6-3). In oxygenated water the SPP size has no significant effect on corrosion..

- Additions of H_2O_2 furthermore suppress the appearance of nodular corrosion in high pressure steam at >470 °C.

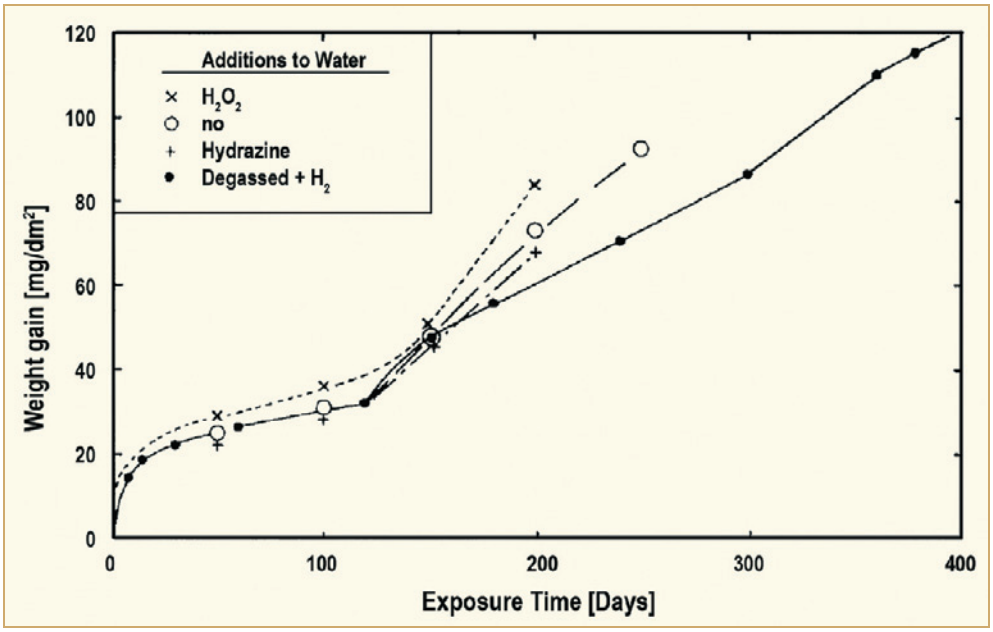

Figure 6-1: Effect of different gases on corrosion of Cold Work and Stress Relieved (CWSR) Zry-4, Lot AP-1 in water at 350 °C [Garzarolli et al, 1989b].

7 Primary failure and secondary degradation – Fuel reliability (Peter Rudling)

The open literature data are provided in the following sections.

7.1 Introduction

7.1.1 Primary failures

During reactor operation, the FR may fail due to a primary cause such as fretting, PCI manufacturing defects, corrosion, etc. (Table 7-1).

Table 7-1: Primary failure causes for LWR fuel during normal operation and Anticipated Operational Occurrences (AOO).

Primary failure cause	Short description
Excessive corrosion	An accelerated corrosion process results in cladding perforation. This corrosion acceleration can be generated by e.g., CRUD deposition (CILC[25]), Enhanced Spacer Shadow Corrosion, (ESSC),[26] (in BWRs), dry-out due to excessive FR bowing.
Manufacturing defects	Non-through-wall cracks in the fuel cladding developed during the cladding manufacturing process. Defects in bottom and/or top end plug welds. Primary hydriding due to moisture in fuel pellets and or contamination of clad inner surface by moister or organics. Too large a gap between the FR and the SG supports (poor SG manufacturing process) leading to excessive vibrations in PWR fuel causing fretting failures. Chipped pellets may result in PCI failures both in liner and non-liner fuel.
PCI	PCI – an iodine assisted SCC phenomenon that may result in fuel failures during rapid power increases in a FR. There are three components that must occur simultaneously to induce PCI and they are: 1) tensile stresses – induced by the power ramp, 2) access to freshly released iodine-occurs during the power ramp, provided that the fuel pellet temperature becomes large enough and 3) a sensitised material – Zircaloy is normally sensitive enough for iodine stress-corrosion cracking even in an unirradiated state.
Cladding collapse	This failure mechanism occurred due to pellet densification. This failure mode has today been eliminated by fuel design changes and improved manufacturing control.
Fretting	This failure mode has occurred due to: Debris fretting in BWR and PWR Grid-rod fretting – Excessive vibrations in the PWR FR causing fuel failures. This situation may occur for example due to different pressure drops in adjacent FAs causing cross-flow. Baffle jetting failures – Related to unexpectedly high coolant cross-flows close to baffle joints.

[25] CILC – an accelerated form of corrosion that has historically resulted in a large number of failures in BWRs. Three parameters are involved in this corrosion phenomenon, namely: 1) Large Cu coolant concentrations as a result of e.g., aluminium brass condenser tubes, 2) Low initial fuel rod surface heat flux – occurs in Gd rods and 3) Fuel cladding that shows large initial corrosion rates- occurs in cladding with low resistance towards nodular corrosion.

[26] This corrosion phenomenon resulted recently in a few failed rods. The mechanism is not clear but seems to be related to galvanic corrosion. This corrosion type may occur on the fuel cladding in contact or adjacent to a dissimilar material such as Inconel. Thus, this accelerated type of corrosion occurred on the fuel cladding material at spacer locations (the spacer springs in alloy BWR fuel vendors fuel are made of Inconel). Water chemistry seems also to play a role if the fuel cladding material microstructure is such that the corrosion performance is poor. Specifically coolant chemistry with low Fe/(Ni-Zn) ratio seems to be aggressive (provided that the cladding material shows poor corrosion performance. A fuel cladding material with good corrosion resistance does not result in *ESSC*, even in aggressive water chemistry.

The failure statistics during 1980-2008 in US PWRs and BWRs are shown in Figure 7-1. About eight BWR 4 and 5 units in the U.S. experienced CILC corrosion failures during the period from 1978 to mid-1980s [Cheng et al, 2009]. *There were three factors involved in these failures: water chemistry more specifically high Cu (and Zn) concentrations in the FW due to condenser tubes made of aluminium brass, fuel cladding microstructure (large SPPs resulting in susceptibility to nodular corrosion) and power history (mostly Gd-rods experienced CILC failures).*

The CILC fuel failure mechanism was eliminated by process improvement of the Zircaloy-2 cladding to minimize nodular corrosion susceptibility and, in most cases, replacement of brass condenser tubes with SS or titanium alloy.

Figure 7-1 shows however, that during the last decade, four BWR units, in the U.S. experienced corrosion and CRUD induced fuel failure with similarities to the earlier CILC failures since the same three factors involved in the CILC failures were also involved in the recent CILC-type failures, namely: 1) water chemistry, 2) fuel cladding microstructure (fuel claddings with low Sn contents and Fe contents showed highest corrosion rates) and 3) power history (high power rods showed more corrosion than low power rods). However, in the most recent CILC-type failures, the dominant factor by far was the water chemistry.

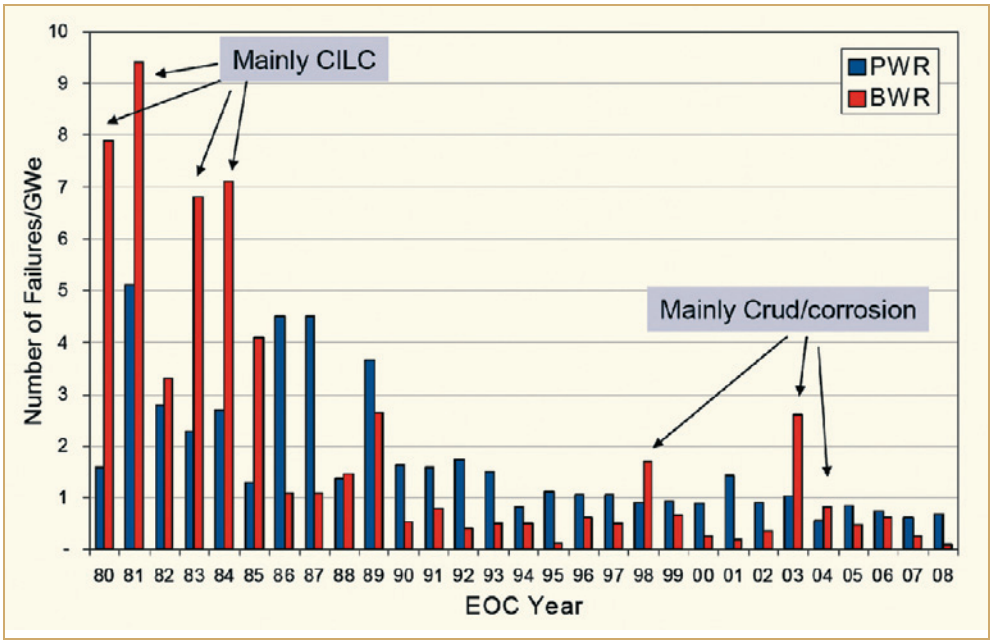

Figure 7-1: Number of failed FAs in all US LWR. This figure shows the US industry annular average fuel failure rates in number of FA per gigawatt electricity produced or roughly per unit for both BWRs and PWRs [Cheng et al, 2009].

In PWRs the primary contributor to failure rates remains GTRF; however, experience with new grid designs appears to be promising. During the last years it was noteworthy that some PCI-suspect failures were also experienced at three B&W-designed PWR plants following the movement of Axial Power Shaping Rods (APSRs) even though their calculated stress levels remained within the permissible range.

In the European BWRs debris fretting is one of the major failure causes. Debris filters in the BWR fuels do not eliminate the debris fretting failures while the debris filters seems to be efficient in the PWRs.

Table 7-2 and Table 7-3 provide key data for some of the most recent fuel-failure cases.

Table 7-2: Summary of previous PWR failure key events, see previous ZIRAT/IZNA-reports for details.

Nuclear unit	Type of primary failure	Comment
TMI-1, Cy 10, 1995	Nine high peaking FRs, Zr-4 Cladding, failed after 122 days of operation. CRUD/corrosion related failures.	• All failed and degraded pins reportedly had Distinctive CRUD Pattern (DCP)[27]. • High peaking factors, thermal-hydraulic conditions. Calculations indicated that no boiling should have occurred on the pins with DCP, although the pins with DCP were calculated to have a slightly higher temperature. • Water chemistry (low pH at Beginning of Cycle (BOC), pH < 6.9, max LiOH 2.2 ppm). • Some, Axial Offset Anomaly (AOA) effect was found reaching a maximum in the middle of cycle 10. • The source of the CRUD could not be determined. The CRUD sampling showed that the nickel-to iron ratio was in the range 1.25 to 16.7, which was reportedly somewhat lower than in previous investigations.
Seabrook, Cy 5, 1997	Five one-cycle ZIRLO rods failed. CRUD/corrosion related failures.	• Longer cycle in transition to 24-month cycle. • Possibly CRUD-induced overheating resulting in substantial nucleate boiling.

[27] This acronym implies that the fuel inspection revealed CRUD deposits on the fuel rod and that the deposits were uneven in the rod circumference.

8 Cladding performance under accident conditions LOCA and RIA (Peter Rudling)

8.1 Loss-of-coolant accident (LOCA)

8.1.1 Introduction (Alfred Strasser)

The design basis LOCA is the double-ended, or guillotine, break of one of the cold, main coolant pipes of a PWR or one of the intake pipes to the recirculation pump of a BWR.

The LOCA process starts by the decrease and ultimate loss of coolant flow at the same time that the reactor is depressurized (Figure 8-1). The loss of coolant flow decreases heat transfer from the fuel, increases the fuel temperature and causes a significant temperature rise of the cladding. The decrease in system pressure causes a pressure drop across and a hoop stress in the cladding. The result is the plastic deformation, or *ballooning* of the cladding. The extent of the ballooning is dependent on:

- Creep strength of the cladding.
- Stress in the cladding and the corresponding strain rate.
- Temperature and the rate of temperature increase.

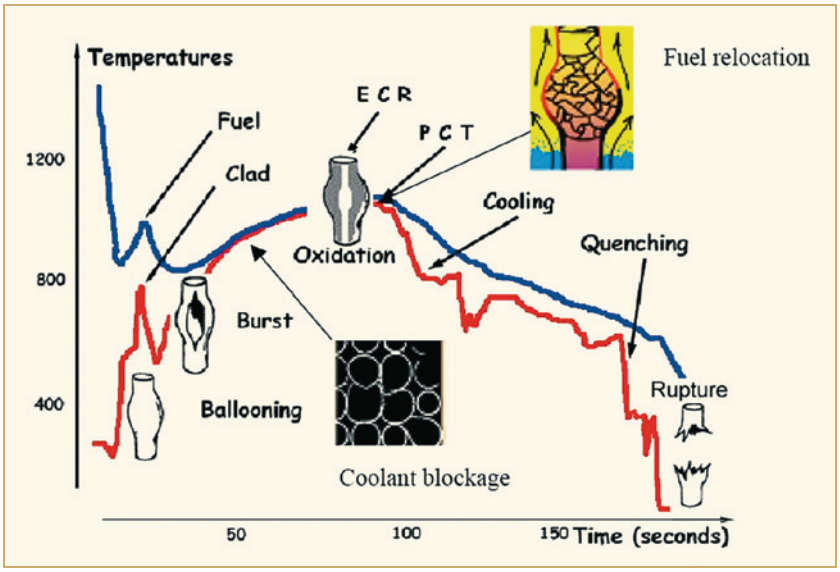

Figure 8-1: Typical LOCA in a PWR.

Depending on the temperature, the cladding ductility and the rod internal pressure, the cladding will either stay intact or may burst. Ballooning of the cladding can result in coolant blockage and reduce fuel coolability. The main objective of the LOCA criteria established by the regulators is to maintain core coolability.

The increasing temperatures and steam will cause the intact cladding to *oxidize* on the OD and the burst cladding to oxidize on both the OD and ID (two sided oxidation) until the ECCS is activated and the water quenches the cladding. The oxidation at the high LOCA temperatures will increase the oxygen and hydrogen content in the cladding, reducing its ductility and resistance to rupture. The process and final structure of the cladding after a LOCA cycle is shown on Figure 8-2.

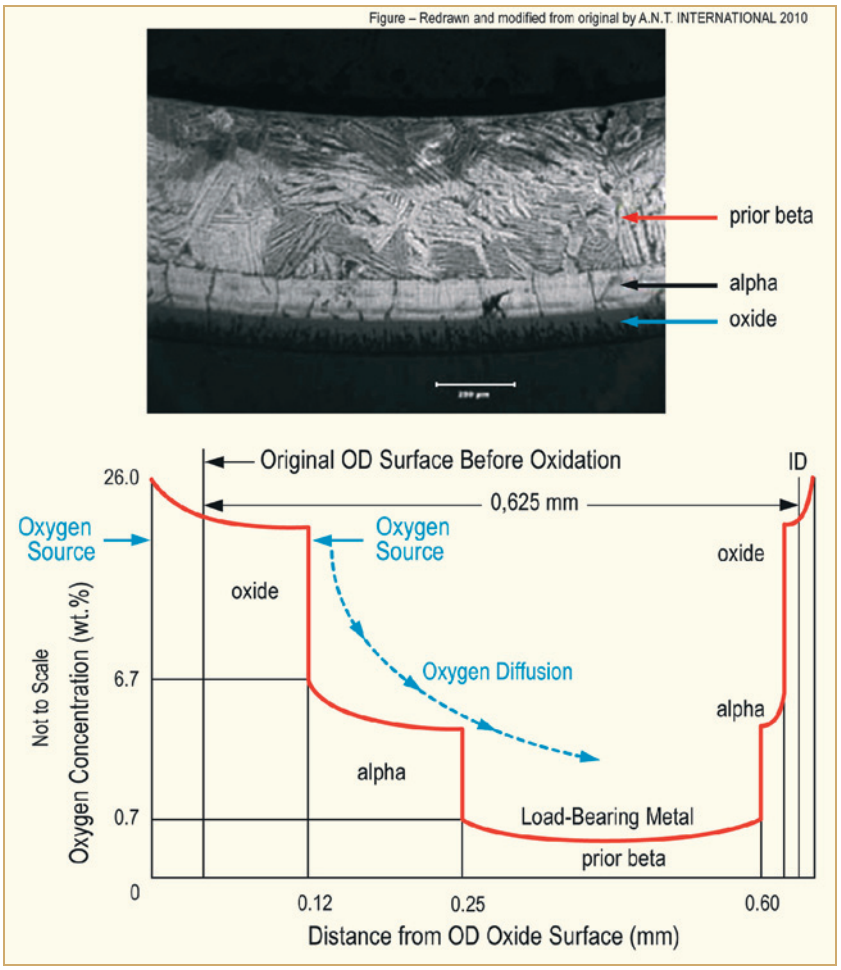

Figure 8-2: Structure of oxidized cladding.

First, the high water and steam temperatures increase their reaction rates with the cladding and increase the conversion of the cladding surface into thicker ZrO_2 films.

As the LOCA temperature passes the levels where α→β transformations start and finish, shown in Figure 8-3 for Zircaloy-4 and M5, the resulting structure consists of:

- The growing ZrO_2 layer.
- A brittle zirconium alloy layer with a very high oxygen content which stabilizes the α phase, formed by diffusion of oxygen from the oxide layer.
- The bulk cladding, which is now in the β phase, has a high solubility for hydrogen; the hydrogen picked up by the cladding from the water-metal reaction increases the solubility of oxygen in the β layer.

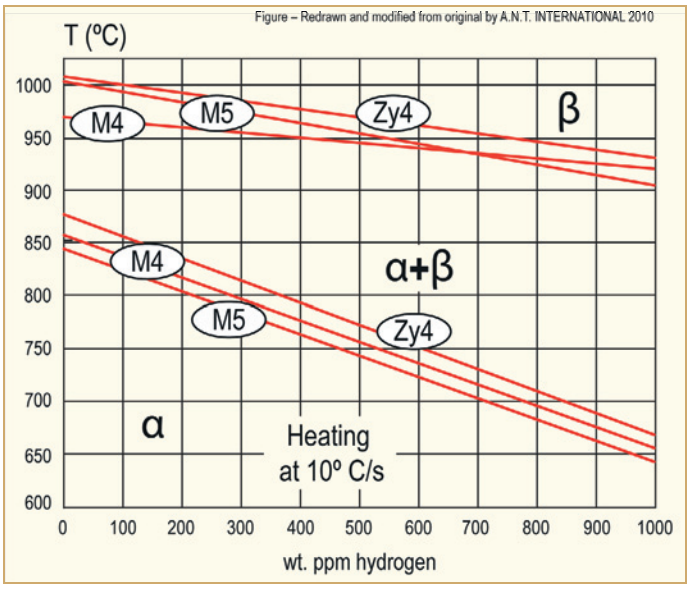

Figure 8-3: The α/β phase transformation temperatures of Zry-4, M4 and M5 alloys as a function of the hydrogen content for a heating rate of 10 °C/s [Brachet et al, 2002].

- The ZrO_2 and oxygen stabilized α layers grow with continued diffusion of oxygen and hydrogen from the water reaction. The increasing amount of oxygen convert some of the β phase to oxygen stabilized α phase with the concurrent shrinkage of the β phase. The remaining β phase cladding wall thickness is transformed to α phase, or "prior β phase", on cooling and is the only structural part of the cladding that can insure its integrity.

The sources and role of hydrogen in the embrittlement of the cladding includes hydrogen from the corrosion reaction during normal operation and hydrogen from the reaction with the LOCA steam. In addition hydrogen increases the solubility of oxygen in the β phase at HTs and oxygen, in combination with hydrogen, are then the two major elements that cause cladding embrittlement by the growth of the α layer and the shrinkage of the structural, prior β layer.

Integrity of the cladding is based on the properties of the former β zone, since the ZrO_2 and oxygen stabilized α zones are too brittle to sustain a load. The embrittlement criteria are based on properties of the prior β layer measured on post-simulated LOCA tests of unirradiated Zircaloy-4, by RCTs [Hobson & Rittenhouse, 1972] and related to oxidation, or ECR, calculated by the Baker-Just equation. It should be noted that the oxide thickness of the samples were never actually measured during those tests, so that the current ECR criteria depend on their relationship to the use of the Baker-Just equation. Modification of this relationship by revised criteria are under discussion with the regulators.

Since the mechanical properties of the prior β zone could change as a function of extended BU and increased oxygen and hydrogen contents, the NRC is evaluating the effects on its properties and the potential need for changing the criteria. Their objective is to make the LOCA criteria material independent, and perhaps independent of % ECR while maintaining the Peak Cladding Temperature (PCT) as discussed subsequently.

9 Fuel performance during intermediate storage

9.1 Introduction (Charles Patterson)

As of mid-2010, about 225 000 tons of Spent Nuclear Fuel (SNF) is stored around world [Sokolov, 2010]. This fuel is being stored in wet and dry conditions in reactor pools and interim storage facilities without major incidents. Storage is, however, only a temporary step in the overall fuel cycle; the fundamental issue of whether the SNF is a resource to be recycled or waste to be disposed of after ageing remains unresolved.

Approaches to the fuel cycle vary among countries with nuclear power programs [Kakodkar, 2010]. Many countries have explicitly or implicitly (by indecision) adopted an open fuel cycle, shown schematically in (Figure 9-1), in which SNF will be disposed of in a permanent repository without recycling. Other countries have implemented or are developing recycling programs which are shown schematically in (Figure 9-2) and (Figure 9-3); e.g., Belgium, China, France, India, Japan, Russia and the United Kingdom. In both cases, capabilities for the final disposal of SNF and related High Level Wastes (HLW) are needed.

Currently, large scale, commercial repositories for SNF and HLW are unavailable. Most countries that generate nuclear power are in the process of developing criteria, designs and sites for the permanent disposal of SNF. As indicated in (Table 9-1), however, operating repositories have yet to become licensed realities. Meanwhile the pools at the nuclear plant sites are filling with spent fuel and the utilities are transferring the spent fuel from the pools to dry cask storage sites that are located, mostly, at the plant sites but also at remote storage facilities. Exceptions are the central, large intermediate pool facilities that serve all the plants in Sweden (CLAB facility) and all the plants in Finland (KPA-STORE). The lack of a licensed permanent fuel repository in any country has placed total reliance on intermediate storage. As a result dry storage has become a major activity and business component of today's back-end fuel strategies.

The importance of dry storage in back-end fuel strategies is due to a combination of factors. As noted above, the absence of permanent, geologic repositories combined with limited, in-pool storage capacity at reactor sites has forced the use of dry storage technology in countries that utilize a once-through, direct-disposal fuel cycle, (Figure 9-1). Note capabilities for interim storage will be needed even after permanent repositories become available because of storage limitations at existing reactor sites and likely constraints on decay heat in the repositories.

Table 9-1: Status of geologic repositories

Country	National decision	Status	Operational target date
Finland	Geological Repository	Site selected; licensing underway	2020
Sweden	Geological Repository	Site selected; licensing underway	2020
USA	Geological Repository	Yucca Mt. suspended in 2009 Alternates being discussed[35]	Unknown
France	Geological Repository	Facility for HLW and transuranics under development	2025
Germany	Geological Repository		2030
Japan	Geological Repository		2030
Switzerland	Geological Repository		2040
UK	Geological Repository	Siting initiated Three communities interested	
Canada	Geological Repository	Siting expected to start in 2010	≥2035
Belgium	No decision	R&D	R&D
Spain	No decision	R&D	R&D

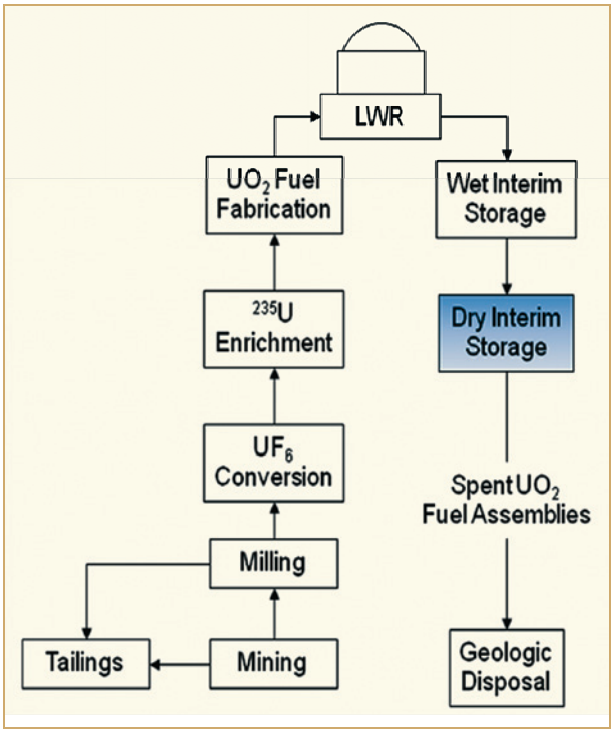

Figure 9-1: Schematic diagram of a once-through fuel cycle. LWR = Light water reactor, but also includes other thermal reactors.

[35] The Waste Isolation Project in New Mexico, USA completed 11 year of successful operation in May, 2010. This facility is a geologic repository for transuranics and other HLW from military programs. It is not being used for commercial SNF.

Economic considerations and capacity imbalances also contribute to the storage of spent UO_2 fuel in countries that have commercial recycling capabilities. That is, dry storage offers a means of delaying reprocessing and recycling operations until the cost of fuel fabricated from virgin uranium or from highly-enriched, weapons-grade uranium justifies the recycling process. Dry storage also offers a means for balancing differences among the inventory of SNF, the capacity to reprocess irradiated fuel and the capacity to recycle the resulting plutonium as MOX fuel in the existing fleet of thermal-spectrum reactors.

It should be noted that, in the absence of permanent geologic repositories, dry storage is also an inherent element of a reprocessing fuel cycle. The build up of actinides such as neptunium, americium and curium typically limit recycling to a single pass through a LWR. As shown in (Figure 9-2), this leads to the storage and disposal of spent, MOX assemblies in addition to the high level waste that comes from the initial reprocessing operation. Recycled fuel generates more decay heat at a given discharge exposure than once-through fuel because of differences in the concentrations of radionuclides. Recycled fuel therefore requires longer decay time to reach a the heat generation rates typically postulated for geologic storage. So, dry storage is common to both once-through and single-recycle fuel cycles.

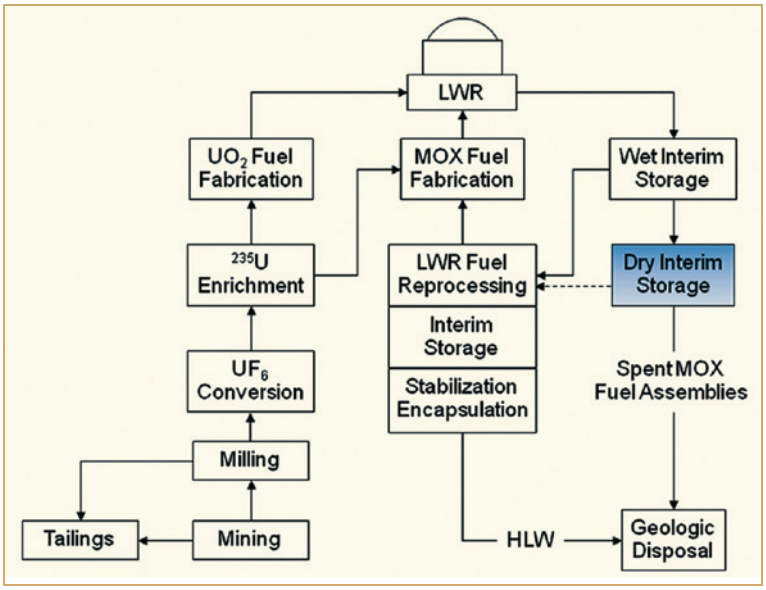

Figure 9-2: Schematic diagram of a once-through, reprocessing fuel cycle. HLW = Waste with high levels of radioactivity. MOX = Fuel consisting of MOXs of uranium and plutonium. LWR = Light water reactor, but also includes other thermal reactors.

In principle, closed fuel cycles such as that shown in (Figure 9-3) can eliminate the need for dry storage. Reprocessing of spent fuel and the partitioning of transuranic nuclides (e.g., Pu, Np, Am, Cm), short half-life fission products (e.g., Cs, Sr) and long-lived fission products (e.g., Tc) are expected to reduce the volume of high level waste by a factor of ten relative to the direct disposal of SNF [Pereira et al, 2006]. The transmutation of the transuranics and selected fission products by means of (fast) reactors with high-energy neutrons or accelerator-based devices is intended to convert these high activity products to stable or short-lived nuclides. The overall effect of reducing the decay heat should allow for geologic disposal within a relatively short interval of time.

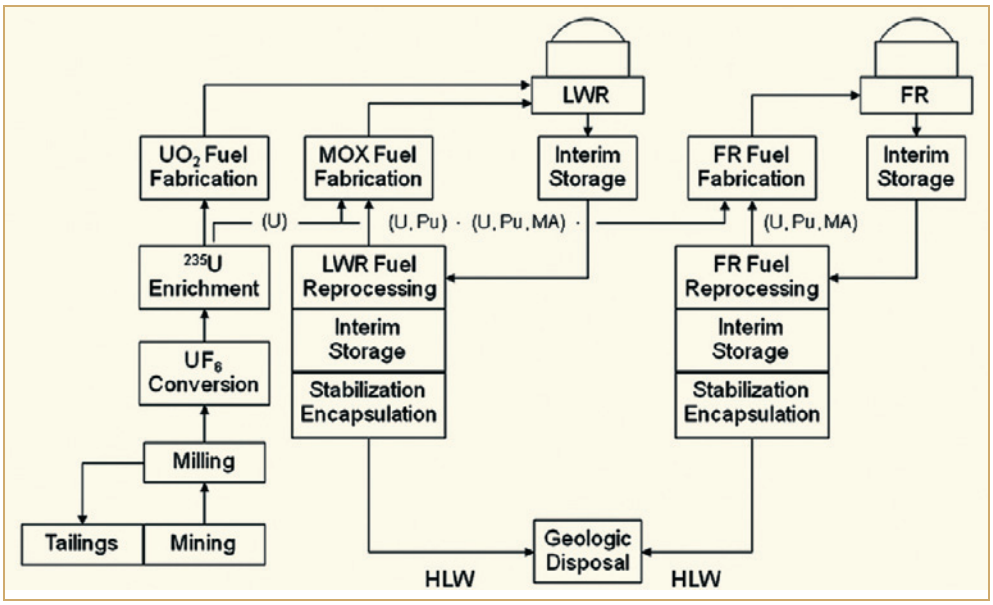

Figure 9-3: Schematic diagram of closed fuel. FR = Fast reactor (transuranic "burner", as shown, or "breeder"). HLW = Waste with high levels of radioactivity. MA = Minor actinides (Np, Am Cm). MOX = fuel consisting of MOXs of uranium and plutonium. LWR = Light water reactor, but also includes other thermal reactors.

In practice, however, the time needed for commercial development of closed fuel cycles and the current extent of political, social and financial support for such activity appears to require the continued use of dry storage through the near-to-intermediate future [OECD NEA, 2009]. Interim storage times in excess of 100 years are now being considered [Kakodkar, 2010] and [Einziger, 2010].

Dry storage of SNF is a relatively mature technology, which has emerged as the consensus, near-term method in most countries that generate electricity by means of nuclear power, [Bunn et al, 2001]. As of 2010, SNF elements from commercial power plants and from research reactors have been stored in a dry state for nearly 30 years and 40 years, respectively [IAEA, 2003]. This experience involves fuel from a wide range of reactor types; e.g., CANDU, HWR, PWR, BWR, VVER-440, VVER-1000, RBMK, MAGNOX and the HTGR. Storage systems include vaults, concrete canisters, steel-lined concrete containers and casks of various configurations, including dual-use containers intended for both transportation and storage. The overall process has been well received by the affected communities and political entities and is being applied by an increasing number of reactor operators [Cohen, 2009]. Although currently well established, the technology, equipment and regulations associated with dry storage continue to evolve with changes that are typically intended to increase storage capacities and storage times; i.e., increase the number of assemblies per container along with allowable exposures, activities and heat loads and increase the time during which SNF will be held in interim storage.

9.5 Criticality considerations (Charles Patterson)

9.5.1 BU credit

Provisions for applying BU credit in the design and loading of dry storage containers are included in the SRP (NUREG-1536, Rev. 1a). Developments in the areas of BU credit and accidents reported in open literature remain essentially unchanged relative to the summary in the ZIRAT13/IZNA8 Annual Report [Strasser et al, 2008c].

9.5.2 Source term definition

The source term to be used for the analyses of radioactive containment of spent fuel casks during storage and transportation is defined in the USA by NRC's NUREG/CR-6487 and NUREG-1536, Rev. 1a. Since the values in these documents were based on the properties of fuel at exposure levels of <45 GWD/MT, a new analysis was made by the NRC to extend the boundary to the current peak licensed exposure of 62.5 GWD/MT peak rod average [Einziger, 2007]. The requirements remain the same as discussed in the ZIRAT13/IZNA8 Annual Report [Strasser et al, 2008c].

9.5.3 Effect of accidents on fuel rods

Fuel rod buckling has been analyzed to evaluate the fuel rod integrity under accident conditions, specifically bottom end drop impact and centre of gravity over corner impact after a 9m (30 ft.) drop. Past analyses by Livermore and Sandia Laboratories have assumed that 90% of the pellet stack is not bonded to the cladding and is supported independently without interacting with the cladding. The NRC has disputed this and has shown that the unattached fuel column fully participates in the buckling process [Bjorkman, 2007].

The model involves a concentric fuel column within a cladding column. The columns can move past each other axially and support their own weight. The two columns are constrained to deform together in what is called "lateral displacement compatibility" and the fuel column must remain in the cladding column. The inertia loads on the fuel and cladding columns will cause the rod to buckle while maintaining lateral displacement compatibility.

The study concluded that the critical buckling load depended on the weight of the fuel and the weight of the cladding columns and that 100% of the fuel participated in the buckling load. Considering only the fuel that is bonded to the cladding in the inertial loading can overestimate the critical buckling load by as much as a factor of five.

The potential for and extent of fuel rod breakage in a cask transport accident was analyzed in an EPRI sponsored study to extend the available data to high BU fuels [Rashid et al, 2006]. The model was for a cask with 24 17x17 PWR assemblies irradiated to about 65 GWD/MT and Zircaloy-4 cladding with 600 ppm hydrogen. A side drop accident was chosen because prior studies by Sandia Laboratories found that this was more damaging than the end or corner drop accidents. Follow-on evaluations to this work have been reported by EPRI and ANATEC [Raschid & Machiels, 2010].

The three previously identified failure modes are represented in (Figure 9-70). Mode I, transverse tearing, and Mode II, rod breakage, were the subject of these evaluations. The dynamic forces affecting these failure modes are the bending moments and the axial tensile forces. The magnitude of the forces depend on the position of the assembly in the cask, the position of the fuel rod in the assembly and the axial position on the rod. The maximum bending moments and axial tensile forces occur at the centre grid.

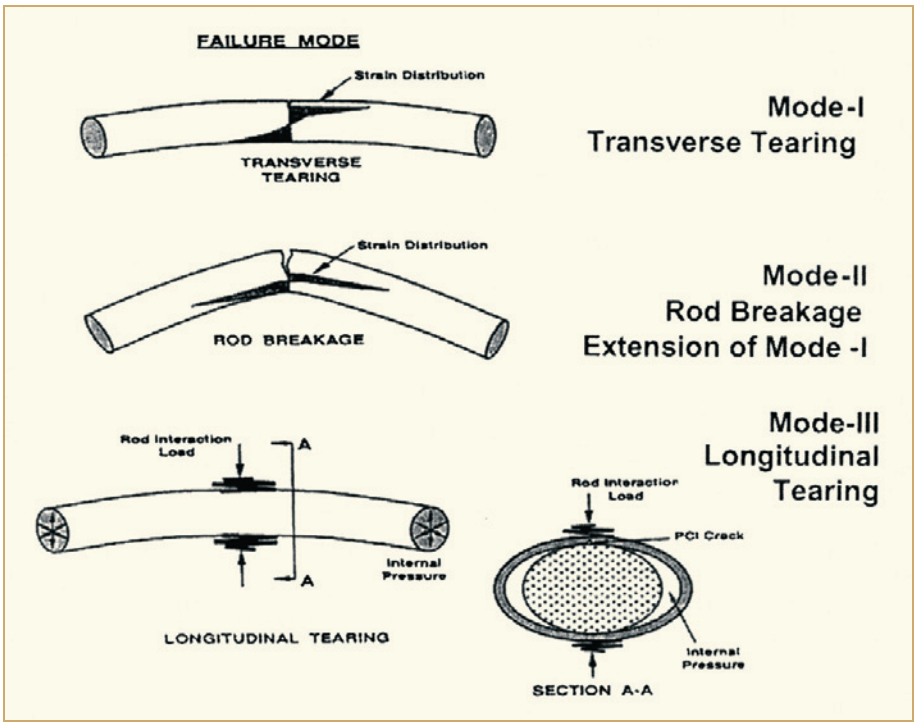

Figure 9-70: Possible modes under cask drop in horizontal orientation [Sanders et al, 1992].

A FEMA analysis with the ABAQUS code evaluated the Mode I/Mode II failure sequence in the fuel rods in three different assemblies. Cladding fracture by Mode I could lead to a through wall fracture, but would constitute a pinhole failure that would not lead to fuel reconfiguration. Continued tearing azimuthally could lead to a guillotine break; however the authors showed that only a partial Mode II failure would happen and that a guillotine break could not occur. The peak values for failure initiation were 1200 lb. for the axial force and 150 in-lb for the bending moment. About 2.5% of the rods exceeded the axial force limit and 75% of the rods exceeded the bending force limit. Since the axial force is the dominant driving force the progression toward failure stops when the axial force drops to zero.

The study concluded that a maximum of 2.5% of the rods in a 24 assembly transport cask would experience partial Mode II tears (< 2 mm wide) with a similar or slightly higher % experiencing transverse tearing. No guillotine break is expected.

The failure probability of the longitudinal tearing Mode III was analyzed by probabilistic methods for the high BU fuel analyzed by the study summarized above, [Rashid et al, 2006] and [Raschid & Machiels, 2010]. The probabilistic was done by a combined deterministic/probabilistic approach considering the statistical variations of the important variables that affect the failure probability of Mode III. The ANATECH SED criteria were applied with the CSED as the criterion for cladding failure. The variables that were considered included the fuel column, which plays the primary role in the resistance of the cladding to failure under dynamic pinch forces resulting from the accident. The fuel-clad gap was found to be particularly significant among all the random variables considered as a factor that can potentially promote through-wall fracture.

The conclusions of the analyses were that cladding failure is bi-modal. Failure initiation is at the cladding ID with part-wall damage and a failure probability of <2%. A through wall failure has a probability of 1E-5.

9.5.4 Effect of fire accidents

Regulations in 10CFR71.73 list the hypothetical accidents that a cask has to withstand and this includes exposure to a 30 minute fully engulfing hydrocarbon fuel fire at 800 °C (1475°F) with a cask surface emissivity of 0.9. The current licensed casks meet this criterion in the US. Past analyses have shown that fuel cladding will be exposed to increased creep deformation >570 °C and may rupture >750 °C. Two publications have analyzed the potential effects of exceeding the time and temperature of this DBA on the cladding temperatures.

The effect of exceeding the 30 minute time on cladding temperatures was analyzed by three different FEMA methods [Venigalla & Greiner, 2007]. The ETC model was used developed by [Manteuffel & Todreas, 1994] and was discussed in a previous section on fuel temperatures. It is a one dimensional analytical idealization of radiation and conduction heat transfer in a two dimensional array of heated rods within a stagnant gas. This model has not been shown to be conservative for accident conditions. In the current work, a two dimensional model of a Legal Weight Truck (LWT) cask cross- section with four 15x15 PWR assemblies with heat generating rods are modelled with the FLUENT CFD code. This code models the conduction, natural convection and radiation heat transfer within the fuel regions as well as conduction in the solid regions. The S-CFD code is a model with stagnant gas used to compare with the CFD model with moving gas.

The CFD model analyzed the Code of Federal Regulations DBA first for the centre and corner rods of the assemblies that generated 800 W/assembly. The results in (Figure 9-71) show the results of peak clad temperatures up to 12 hours after the 30 minute fire noted by the dashed line. The clad temperatures keep rising even after the DBA fire is extinguished due to the continuous diffusion of heat from the hotter regions of the cask periphery. The temperature of the fuel rod at the corner rises sooner compared to the centre, since it is close to the hot surface of the cask; however, the centre continues to rise to a maximum of 269 °C in this specific case.

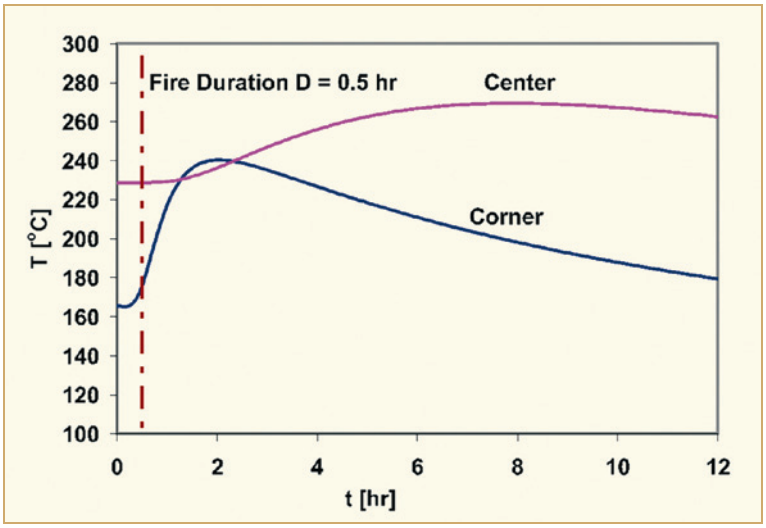

Figure 9-71: Center and corner rod cladding temperature versus time for a CFD simulation with N_2 gas for an 800 °C fire duration of 30 minutes [Venigalla & Greiner, 2007].

The peak post-fire cladding temperatures were analyzed for fire durations of 30 minutes up to 14 hours and are compared in (Figure 9-72) for the three models. Variability between the models can be due to factors beyond basic model differentials, such as the limited number of fuel rod locations monitored and differences in the pre-fire temperatures between the three models. In general one could say that for this specific cask and heat generations a >4 hour DBA fire would lead to extensive creep deformation and a >10 hour fire to potential rupture of the cladding.

10 Potential BU limitations

10.1 Introduction

The potential FA BU limitations related to zirconium alloy components are summarised in this Section. The BU limitations that have actually been reached, but have been or are being extended, are:

- Corrosion limits of Zry-4 in high power PWRs are extended by the alternate use of improved cladding alloys. Improved corrosion performance by the new alloys may allow the utilities to use the added margins, to modify plant operation e.g., to lower fuel cycle cost. However, this modified operation will in most cases result in higher corrosion duty of the zirconium materials. Thus, it is believed that the corrosion may always be limiting for plant operation even with the new type of alloys. Furthermore, the influence of CRUD on corrosion may increase with increasing duty.

- Bowing of PWR FAs contributed in part by irradiation growth, creep and hydriding of Zry-4, has been reduced by improved GT materials (i.e., lower irradiation growth and hydriding rates), reduced assembly hold-down forces, and other mechanical/thermomechanical design changes, but not yet finally eliminated. More complete understanding of irradiation growth and hydrogen uptake mechanisms are desired.

- Bowing of BWR channels, extended by improved manufacturing processes, design changes such as variable wall channel thickness with relatively thicker corners, and in-core channel management programs. More complete understanding of irradiation growth, shadow corrosion and hydrogen uptake mechanisms are desired.

- RIA and LOCA related BU licensing limits are in the process of being assessed by additional experimental data and analyses. It would appear that the current LOCA limits are sufficiently conservative for fuel BUs up to 75 MWd/kgU. The RIA limits (threshold enthalpies) may continue to decrease as a function of BU due to the increase in clad corrosion and hydrogen uptake. More understanding of the relationship between laboratory testing techniques and actual event phenomena are desired.

- The categories of event likely to eventually limit reliably and safely achievable BU levels are outlined below. The zirconium alloy component most sensitive to the limits and potential methods for extending the limits are noted below.

10.2 Corrosion and mechanical properties related to oxide thickness and H pickup

- BWRs: increased uniform and shadow corrosion, oxide thickness spalling, increased HPU, and formation of radial hydrides due to longer residence time, higher power, modern power histories, and water chemistry changes. Current crucial issues are shadow corrosion mechanisms and their effects on channel bow, late increased corrosion and HPU of Zry-2 at high BUs, and formation of radial hydrides, CRUD-chemistry-corrosion interaction, effect of water chemistry impurities, as well as specific effects of NMCA with or without Zn-injection.

- PWRs: increased uniform corrosion, oxide thickness, spalling, and new Zr alloys due to longer residence time and higher Li, higher power, more boiling. The development of new Zr-alloys is still ongoing. The database for several of the new alloys is still limited. Zr-Nb alloys are occasionally affected by accelerated corrosion due to surface contaminations and/or boiling. Welding of the new alloys may need improved processes (Zr-Nb alloys) and chemical compositions between dissimilar metals such as e.g. ZIRLO and Zry-4 may result in inferior corrosion resistance. Since the cladding temperatures at these elevations in the core are currently significantly lower than the peak temperatures, the effect on corrosion is minimized.

- Decreased ductility and fracture toughness as consequence of the increased HPU during any situation (e.g., RIA, PCMI, LOCA and post-LOCA events, seismic event, transport container drop-accident conditions).
- Increased component dimensional change due to higher hydride volume and thick oxide layers.
- Increased corrosion due to impact of hydrides at the cladding outer surface.
- Impact of corrosion and HPU on creep behaviour of fuel claddings during class 1-IV events and during intermediate storage.
- Increased effects of irradiation and hydrides on the fracture toughness of thin-walled zirconium alloy components.

Most sensitive component

Fuel cladding and structural components such as spacers, PWR GTs, BWR channels.

Means of increasing margin for PWR

- Improved knowledge of corrosion and HPU mechanisms.
- Improved alloys with appropriate fabrication processes: ZIRLO, MDA, New Developed Alloy (NDA), and M5/Zr1Nb. DX are another alternative that may be necessary to achieve satisfactory mechanical properties.
- Zr-alloys such as Optimised ZIRLO, Modified MDA, S2, Modified E635 with reduced Sn content in comparison to the original composition of ZIRLO, MDA, NDA and E635 are being explored.
- Change to enriched B soluble shim to reduce Li. There is however a fear that enriched B would increase AOA potential, i.e., more absorption per g. B, even though there may be less B.
- Improved water chemistry and CRUD control.
- Increase corrosion resistance of steam generator materials.
- Increase understanding and quantification of deformation mechanism, including modes of dislocation channelling.

Means of increasing margin for BWR

- Improved knowledge of corrosion, shadow corrosion and HPU mechanisms at high BUs.
- Modification of manufacturing processes (to get optimum sized, more stable SPPs).
- Possible use of Zry-4 fuel channels for controlled positions.
- Improved alloys under development.
- Improved water chemistry and CRUD control.
- Increase understanding and quantification of deformation mechanism, including modes of dislocation channelling

10.3 Dimensional stability

- Increased dimensional changes of components and differential dimensional changes between them resulting in reduced FR spacing or even rod contact, GT bowing, FA bowing, spacer cell and envelope dimensions, BWR fuel channel and PWR FA bow may result in:
  - Decreased thermal margins (LOCA and dry-out).
  - Control rod insertion difficulties (safety issue).

Most sensitive component

Potentially all zirconium alloy components, but currently Zircaloy PWR GTs and BWR channels. Also BWR spacers have occasionally increased so much in dimensions that unloading of the assembly from the outer channel was very difficult.

Means of Increasing margin for PWRs

- Alloys with lower growth and hydriding rates for GTs – ZIRLO, M5, E635 (Anikuloy).
- Modified mechanical design to provide lower hold-down forces, stiffer assemblies, etc.
- Refinement of the understanding of the effects of corrosion and hydriding at moderate and high BUs.
- Beta-quenched material after the last plastic deformation step during manufacturing. (Beta-quenched materials do normally, however, show higher corrosion rate and lower ductility. These properties might be improved by an appropriate final heat-treatment in the alpha-phase. Also applies to BWR materials control of texture (close to ideal isotropy) is critical for good performance at high BUs).
- Increased understanding and data on effects of material chemistry and microstructure on irradiation creep and growth.

Means of increasing margin for BWRs

- Uniform microstructure and texture throughout the flow channel.
- Use of lower growth material, such as beta-quenched material in as-fabricated step, NSF or other Nb-modified zirconium alloys.
- Channel management programs, including assessment of degree of control over specific reactor periods.
- More corrosion and shadow-corrosion resistant material in channels and spacers.
- Increased understanding of basic phenomena driving the channel bow process, including flux and hydrogen-driven processes.
- Lowered hydride pickup and increased uniformity of hydride distribution in channels and spacers through heat treatment and alloy choice.
- Increased understanding and data on effects of material chemistry and microstructure on irradiation creep and growth.

11 References

Abe H. and Takeda K., *Development of advanced Zr alloy cladding tube (S2) for PWR*, Annual Meeting of the AESJ and private information, 2006.

Adamson, R. B., *Cyclic Deformation of Neutron Irradiated Copper*, Phil. Mag. 17, pp. 681, 1968.

Adamson R. B. and Bell W. L., *Effects of Neutron Irradiation and Oxygen Content on the Microstructure and Mechanical Properties of Zircaloy*, Microstructure and Mechanical Behavior of Materials, Proceedings: Int'l Symposiums, Xian, China, October, 1985, EMAS, pp. 237-246, Warley, UK, 1986.

Adamson R. B., Wisner, S. B., Tucker, R. P. and Rand. R. A., *Failure Strain for Irradiated Zircaloy Based on Subsized Specimen Testing and Analysis*, The Use of Small-Scale Specimens for Testing Irradiated Material, ASTM STP 888, W. R. Corwin and G. E. Lucas, Eds., American Society for Testing and Materials, 171-185, Philadelphia, 1986.

Adamson, R. B. and Lewis, J. L., Abstracts, Ninth International Symposium, Zirconium in the Nuclear Industry, Kobe, Japan, 1991.

Adamson R. B., *Alloy for improved corrosion resistance of nuclear reactor components*, Patent EP0735151B1, 1996.

Adamson R. B., *Effects of Neutron Irradiation on Microstructure and Properties of Zircaloy*, Zirconium in the Nuclear Industry; Twelfth International Symposium, ASTM STP 1354, pp. 15-31, West Conshohocken, PA, 2000.

Adamson R. B. and Rudling P., *Mechanical Properties of Zirconium Alloys*, ZIRAT6/IZNA1 Special Topics Report, ANT International, Skultuna, Sweden, 2001/2002.

Adamson and Cox, *Impact of Irradiation on Material Performance*, ZIRAT10/IZNA5 Special Topics Report, ANT International, Skultuna, Sweden, 2005/2006b.

Adamson R. B. et al, *ZIRAT10/IZNA5 Annual Report*, ANT International, Skultuna, Sweden, 2005/2006.

Adamson R. B., *Recovery of Irradiation Damage by Posts-Irradiation Thermal Annealing-Relevance to Hydrogen Solubility and Dry Storage Issues*, EPRI Technical Report 1013446, June 2006.

Adamson R. B. et al, *ZIRAT11/IZNA6 Annual Report*, ANT International, Skultuna, Sweden, 2006/2007a.

Adamson R. et al., *Pellet-Cladding Interaction (PCI and PCMI)*, ZIRAT11/IZNA6, Special Topics Report, ANT International, Skultuna, Sweden, 2006/2007.

Adamson R. B. et al, *ZIRAT14/IZNA9 Annual Report*, ANT International, Skultuna, Sweden, 2009a.

Adamson R. B, Garzarolli F. and Patterson C., *In-Reactor Creep of Zirconium Alloys*, ZIRAT14/IZNA9 Special Topical Report, ANT International, Skultuna, Sweden, 2009b.

Akhtar A. and Teghtsoonian A., *Basal Slip in Zirconium*, Acta Met., Vol. 19, pp. 655, 1971.

Alvarez Holston A-M. et al., *A combined approach to predict the sensitivity of fuel cladding to hydrogen-induced failures during power ramps*, Meeting on LWR Fuel Performance), Paper 127, Orlando, FL, 2010.

Alyokhina S., *Investigation of thermal processes at dry storage of spent nuclear fuel*, Presented at the International Conference on Management of Spent Fuel from Nuclear Power Reactors, IAEA Vienna, 31 May – 4 June 2010, Vienna, Austria, 2010.

Amaya M., Nakamura J., Fuketa T. and Kosaka Y., *Relationship Between Changes in the Crystal Lattice Strain and Thermal Conductivity of High Burnup UO_2 Pellets*, Journal of Nuclear Materials, Vol. 396, pages 32-42, 2010.

Ambler J. F. R. and Coleman C. E., *Acoustic emission during delayed hydrogen cracking in Zr-2.5 wt% Nb alloy*, Proc. Second International Congress on Hydrogen in Metals), Paper 3C10, Pergamon Press, Oxford, 1977.

Ambler J. F. R., *Effect of direction of approach to temperature on the delayed hydrogen cracking behavior of cold-worked Zr-2.5Nb*, Zirconium in the Nuclear Industry – Sixth International Symposium, ASTM STP 824, D. G. Franklin and R. B. Adamson, Eds., American Society for Testing and Materials), 653-674, Philadelphia, PA, 1984.

Amouzouvi K. F. and Clegg L. J., *Effect of heat treatment on delayed hydride cracking in Zr-2.5 wt pct Nb*, Met. Trans. A., 18A), 1687-1694, 1987.

Andersson T. and Wilson A., *Ductility of Zircaloy Canning Tubes in Relation to Stress Ratio in Biaxial Testing*, In: Zirconium in the nuclear industry: 4th Int. Symp. ASTM STP-681, J. H. Schemel and T. P. Papazoglou (Eds), American Society for Testing Materials, pp. 60-71, 1979.

Anon, The Boiler and Pressure Vessel Code, American Society of Mechanical Engineers, Section VIII, Division I, Subsection C, UNF-56, (d), p. 183, 1992.

Anon, Canadian Standards Association, Technical requirements for in-service evaluation of zirconium alloy pressure tubes in CANDU reactors, N285.8-05, 2005.

Aomi M. et al., *Evaluation of Hydride Reorientation Behavior and Mechanical Property for High Burnup Fuel Cladding Tube in Interim Dry Storage*, Presented at the ASTM 15th International Symposium on Zirconium in the Nuclear Industry, June 2007, Sunriver, Oregon, USA., 2007.

Aomi M. et al., *Evaluation of hydride reorientation behavior and mechanical properties for high-burnup fuel-cladding tubes in interim dry storage*, J. ASTM International, 5, Paper ID JAI101262, 2008.

Aomi M. et al., *The Hydrogen Pick-up Behaviour for Zirconium-based Alloys in Various Out-of-pile Corrosion Test Conditions*, Top Fuel 2009, Paper 2077, Paris France, 2009.

Aomi M. et al., *Evaluation of Hydride Reorientation Behavior and Mechanical Properties for High-Burnup Fuel-Cladding Tubes in Interim Dry Storage*, Journal of ASTM International, Vol. 5, Issue 9, Paper ID JAI101262, 2009.

Arborelius J. et al., *The effect of duplex cladding outer component tin content on corrosion, hydrogen pick-up, and hydride distribution at very high burnup*, J. ASTM International, 2, Paper ID JAI12411, 2005.

Armijo J. S., *Performance of failed BWR fuel*, International Topical Meeting on LWR Fuel Performance, West Palm Beach, ANS, 410-422, 1994.

Armijo J. S., Coffin L. F. and Rosenbaum H. S., *Development of zirconium-barrier fuel cladding*, Zirconium in the Nuclear Industry – 10th International Symposium, ASTM STP 1245, A. M. Garde and E. R. Bradley, Eds., American Society for Testing and Materials, 3-18, West Conshohocken, PA, 1994.

Arslan M., Gros J-P., Niquille A. and Marincic A., *MOX in Reactors: Present and Future*, LWR Fuel Performance Conference, Orlando, Florida, September, 2010.

Aulló M., Garcia-Infanta J. and Chapin D., *Post Irradiation Examination of High Burnup Assemblies in Vandellos II*, LWR Fuel Performance Conference, Orlando, Florida, September, 2010.

Barrachina T. et al., *Influence of the Thermal hydraulic to Neutronic Channel Mapping in a 3D REA Analysis with Relap5/Parcs v2.7 at Trillo NPP,* Proceedings of Top Fuel 2009, Paris, France, September 6–10, 2009a.

Barrachina T. et al., *Rod Ejection Accident 3D-Dynamic Analysis in Almaraz NPP with Relap5/Parcs v2.7 and Simtab Cross-Sections Tables*, Proceedings of Top Fuel 2009, Paris, France, September 6–10, 2009b.

Barraclough K. G. and Beevers C. J., *Some observations on the deformation characteristics of bulk polycrystalline zirconium hydride. Part 1. The deformation and fracture of hydrides based on the δ-phase*, J. Mat. Sci., 4, 518-525, 1969.

Barnes R. S., *in Flow and Fracture of Metals and Alloys in Nuclear Environments*, ASTM, Philadelphia PA, pp. 40–67, 1965.

Beck R. L. and Mueller W. M., Nuclear Metallurgy, a symposium on metallic moderators and cladding materials, Vol. VII, 63-66, AIME, New York, 1960.

Bell W. L., *Discussion*, Zirconium in Nuclear Applications, ASTM STP 551, ASTM, pp. 199-120, 1974.

Bement A. L., Jr., *Radiation Effects*, AIME Metallurgical Society Conferences, Vol. 37, W. F. Sheely, Ed., pp. 671, 1967.

Bertsch J., Valance S. and Zubler R., *Crack Resistance Determination of Irradiated Fuel Cladding using the Cladding Tensile Fracture Test (CTFT*), 2010 LWR Fuel Performance Meeting/Top Fuel/WRFPM, Orlando, Florida, paper 047, Sept. 2010.

Bingert J. et al., *Deformation twinning in polycrystalline Zr: Insights from electron backscattered diffraction characterization*, Metallurgical and Materials Transactions A, Volume 33, Number 13, pp. 955-963(9), Publisher: Springer, March 2002.

Bjorkman G., *The buckling of fuel rods under inertia loading*, Paper CO 3/2, SMiRT 19, Toronto, August 2007.

Bondre J. and Guzeyev V., AREVA/TRANSUCLEAR'S NUHOMS MP197 Transportation Package with Higher Burnup and Higher Heat Load Canisters as a Payload, 15th PATRAM Conference, Miami, Florida, October, 2007.

Bouffioux P. and Rupa N., *Impact of Hydrogen on Plasticity and Creep of Unirradiated Zry-4 Cladding Tubes*, Zirconium in the Nuclear Industry: Twelfth International Symposium, ASTM STP 1354, Sabol G. and Moan G., Eds., American Society for Testing and Materials, pp. 399-422, West Conshohocken, PA, 2000.

Bourdiliau B., et al., *Impact of irradiation damage recovery during transportation on the subsequent room temperature tensile behavior of irradiated zirconium alloys*, 16th International Symposium on Zirconium in the Nuclear Industry, ASTM, Chengdu, China, May, 2010.

Brach E. W., *Cladding consideration for the transportation and storage of spent fuel*, USNRC Interim Staff Guidance – 11, Revision 3, Spent Fuel Project Office, 2003.

Brachet J. C., Portier L. and Forgeron T., *Influence of Hydrogen on Content on the α/β Phase Transformation Temperatures*, Zirconium in the Nuclear Industry- Thirteenth International Symposium, ASTM STP 1423, ASTM, pp. 673-701, 2002.